ALMA MATER STUDIORUM
UNIVERSITÀ DI BOLOGNA

ARCHIVIO ISTITUZIONALE
DELLA RICERCA

Alma Mater Studiorum Università di Bologna
Archivio istituzionale della ricerca

Entheseal variation and locomotor behavior during growth

This is the final peer-reviewed author’s accepted manuscript (postprint) of the following publication:

Published Version:
Entheseal variation and locomotor behavior during growth / Mameli, D; Pietrobelli, A; Sorrentino, R; Nicolosi, T; Mariotti, V; Belcastro, MG. - In: JOURNAL OF ANATOMY. - ISSN 0021-8782. - ELETTRONICO. - Early View:(2024), pp. 1-19. [10.1111/joa.14023]

Availability:
This version is available at: https://hdl.handle.net/11585/961802 since: 2024-02-26

Published:
DOI: http://doi.org/10.1111/joa.14023

Terms of use:

Some rights reserved. The terms and conditions for the reuse of this version of the manuscript are specified in the publishing policy. For all terms of use and more information see the publisher's website.

This item was downloaded from IRIS Università di Bologna (https://cris.unibo.it/).
When citing, please refer to the published version.

(Article begins on next page)

29 April 2024

This is the submitted manuscript (Pre-print) of:

Mameli, D., Pietrobelli, A., Sorrentino, R., Nicolosi, T., Mariotti, V., & Belcastro, M. G. (2024). Entheseal variation and locomotor behavior during growth. Journal of Anatomy.

The final published version is available online at: **https://doi.org/10.1111/joa.14023**

Rights / License:

The terms and conditions for the reuse of this version of the manuscript are specified in the publishing policy. For all terms of use and more information see the publisher's website.

This item was downloaded from IRIS Università di Bologna (https://cris.unibo.it/)

When citing, please refer to the published version.

Entheseal variation and locomotor behavior during growth

Mameli Davide[1], Pietrobelli Annalisa[1], Sorrentino Rita[1], Nicolosi Teresa[1,2], Mariotti Valentina[1], Belcastro Maria Giovanna[1]

[1]Department of Biological, Geological and Environmental Sciences, Alma Mater Studiorum University of Bologna, Italy

[2]Department of Cultural Heritage, Alma Mater Studiorum University of Bologna, Italy

Corresponding author: Belcastro Maria Giovanna

E-mail: mariagiovanna.belcastro@unibo.it

Postal address: Department of Biological, Geological and Environmental Sciences, Alma Mater Studiorum University of Bologna, via Selmi 3, 40126, Bologna, Italy

Abstract

Entheses are acknowledged as skeletal markers capable of revealing several biological and behavioral aspects of past individuals and populations. However, entheseal changes (ECs) of juvenile individuals have not yet been studied with a systematic approach. This contribution aims at investigating the morphological changes occurring at the femoral insertion of the *gluteus maximus* and tibial origin of the *soleus* muscles to highlight a potential link between the morphological features of those entheses and skeletal maturity in relation to sex, age and locomotor developmental patterns. The sample consisted of 119 skeletons (age-at-death: 0-30 years) belonging to the Documented Human Skeletal Collection of the Certosa Cemetery (Bologna, Italy). The entheseal variation during the last stages of skeletal maturation in young adults was assessed using existing recording standards. A recording protocol for each enthesis was developed for immature individuals to subdivide the morphological variability into discrete categories. Univariate, bivariate and multivariate statistical analyses were performed to investigate the variation of entheseal morphologies and measurements in relation to bone metrics, degree of epiphyseal closure, sex, age and locomotor developmental patterns. A statistically significant relationship was observed between ECs morphological patterns and age for both entheses, while sexual differences were negligible. A relationship between ECs morphological pattern and locomotor milestones emerged only for the *gluteus maximus*. Even though further testing is needed on other documented skeletal collections, our protocol could be usefully applied in forensic and archaeological fields and serving as important reference for evolutionary investigations.

Keywords

Entheseal Changes; Locomotor Development; Documented Skeletal Collections; Skeletal Maturation

1. Introduction

The entheses are the areas where tendons, ligaments and joint capsules attach to the bone (Benjamin et al., 2002), and represent the only direct evidence of the musculotendinous system on skeletal remains. The entheseal changes (ECs; this term designates all alterations of entheses seen in the skeletal material; Jurmain and Villotte, 2010) have been largely explored in the last decades. The entheses are physiologically subjected to significant mechanical stress, which inevitably leads to some reaction in the bone tissue. Even if the extent to which the mechanical stress influences entheseal morphology with respect to other factors (age, hormonal factors, etc) cannot be ascertained, entheses are widely uses in the attempt to reconstruct biological and behavioral aspects (Dutour, 1986; Hawkey and Merbs, 1995; Kennedy, 1998; Weiss, 2003; Belcastro et al., 2006; Mariotti and Belcastro, 2011; Villotte and Knüsel, 2013; Belcastro and Mariotti, 2017; Belcastro et al., 2020;

Karakostis and Harvati, 2021; Karakostis et al., 2021). However, ECs expression (robusticity and pathological features) has a multifactorial etiology, where the aging process in adulthood is one of the main factors involved (Cunha and Umbelino, 1995; Robb, 1998; Mariotti et al., 2004, 2007, 2009; Villotte, 2009; Alves Cardoso and Henderson, 2010; Villotte, 2009; Villotte et al., 2010; Niinimäki, 2011; Milella et al., 2012; Villotte and Knüsel, 2013). As far as sex is concerned, some dimorphism has been observed in adults, often, but not always, corresponding to a greater entheseal robusticity in males (Mariotti et al., 2007; Alves Cardoso and Henderson, 2010; Milella et al., 2012). Different observational recording standards have been so far developed, but only on bones of adult individuals (e.g., Hawkey and Merbs, 1995; Mariotti et al., 2004, 2007; the Coimbra method by Henderson et al., 2016, 2017), while little attention has been given to the ECs during growth in juvenile skeletons.

Our previous investigations have shown different patterns in some lower limb entheseal morphologies between Neanderthals (Krapina, 130 000 BP and El Sidrón, 49 000 BP) and modern humans (Belcastro et al., 2006; Mariotti and Belcastro, 2011; Belcastro and Mariotti, 2017; Belcastro et al., 2020). Our results showed that the morphological variability of the *gluteus maximus* enthesis exceeded that observed in modern humans, while the variability of the *soleus* was comparable to modern humans'. In detail, we observed a low intrapopulation variability in each Neanderthal sample (despite small sample size) between the adult and juvenile morphology of *gluteus maximus* muscle, and a large intrapopulation variability in modern humans between the adults and juvenile individuals on the same enthesis. Furthermore, we empirically observed that modern juveniles exhibited characteristics that exceeded the variability seen in the adults and the absence of standardized recording systems hindered our ability to quantify these differences. Many entheses in the adults were completely covered by variably developed *mineralized tissue formations* (Villotte et al., 2016), formerly known as crests or ridges (Peterson, 1998; Robb, 1998; Hawkey and Merbs, 1995; Eshed et al., 2004; Mariotti et al., 2007; Milella et al., 2012). Juvenile individuals, on the other hand, systematically presented *surface discontinuities* (like diffuse porosity and furrows) covering the entire entheseal surface, as also previously observed by other authors (Matyas et al., 1990; Wei and Messner, 1996). A recording standard for juvenile entheses has been recently published by Palmer et al. (2023). However, of age (Bly, 1994)the authors just score a set of features already known in the literature (e.g., enthesophytes; cf. Villotte et al., 2016) that could be recorded on any individuals regardless to their age class. On the contrary, in the present work, we specifically investigate the variability of juvenile entheseal morphologysex and , focusing on surface architecture and texture. These features allow to univocally recognize juvenile morphologies. Additionally, we had the possibility to study a much larger sample where most of the age classes are better represented.

Our work is aimed at investigating the entheseal morphometric variability of the femoral insertion of *gluteus maximus* (hereinafter "GM") and tibial origin of *soleus* (hereinafter "SOL") muscles (already studied in the Neanderthal samples) in juvenile individuals in relation to age, sex and locomotor pattern during growth, adding new insights on the biological and biomechanical aspects of bipedalism, from an ontogenetic and evolutionary point of view, already explored in our research group also with other approaches (Sorrentino et al., 2020a, 2020b, 2020c, Figus et al., 2022, 2023; Pietrobelli et al., 2022a, 2022b, 2023; Colombo et al., 2019). In detail, we developed a recording standard method to better classify the entheseal (continuous) variability into discrete classes and verify its applicability in response to the locomotor pattern (detailed below). In this frame, the availability to access to the Documented Human Skeletal Collection (Belcastro et al., 2017, 2022), sampling individuals with known sex and age, allowed us for trying to meet those objectives.

1.1. GM and SOL in locomotion development

GM and SOL muscles are highly involved in human bipedal locomotion. The human gait cycle can be divided into two phases (Whittle, 2006; Neumann, 2009): a stance phase, where the foot is in contact with the ground, and a swing phase, where the foot swings before touching the ground. The GM and the SOL are both involved in the stance phase. Specifically, the GM is involved from the moment the heel contacts the ground (i.e., Initial Contact) and remains active until the moment the heel leaves the ground (i.e., Heel Rise) to promote hip extension; the SOL, instead, contracts during late mid-stance and terminal stance to promote plantar flexion and control dorsiflexion.

During the first six months after birth the infant performs precursory locomotor movements like supine kicking and supported sitting, while weight-bearing on lower limbs is completely absent (Thelen and Fisher, 1982; Thelen et al., 1984). Afterwards, the child goes through a short period (up to 8 months) of dependent/independent crawling and scooting. Infants typically gain a standing position and start cruising towards the end of the first year of life, at first while holding on to objects or caregivers for support and eventually transitioning to independent toddling (Bly, 1994; Adolph et al., 1998). From about one year of life, the toddler goes through various stages of maturation of their locomotor behavior and towards the age of 6 they acquire the mature bipedal gait typical of adults. In the early phases of toddling (i.e., between the ages of 1 and 2 years), children lean on a wide base of support, abducting their thigh and flexing their hip and knee. They point toes outwards and strike the ground with a plantigrade foot (McGraw, 1940; Forssberg, 1985; Hallemans et al., 2003; Hallemans et al., 2006a, b). As a result of a flexed hip and knee, the torso tends to lean forward causing the hip (contralateral to the standing leg) to lift during the swing phase and the pelvis to tilt from side to side (Hallemans et al., 2004; Cowgill et al., 2010). This early form of walking is typically conducted at a slow pace, with small and jerky steps performed in bursts at irregular intervals (Hallemans et al., 2006a). Children at age 3 usually engage in a more mature toddling pattern, with improved gait, narrower and longer steps, and a loading pattern of an initial heel-strike which sees the beginning of the stride with the center of pressure under the calcaneus (Adolph et al., 2003; Ivanenko et al., 2004; Hallemans et al., 2006b; Zeininger et al., 2018; Swan et al., 2020). Finally, around age 6 (on average), a mature, stable, and efficient gait is fully acquired, as a result of the progressive increase in the femoral bicondylar angle (that adducts the knee, positioning the joint under the body's center of gravity) which leads to the correction of the *genu varum* typical of toddlers (Tardieu and Trinkaus, 1994; Swan et al., 2020).

From the locomotor behavior illustrated above, during growth, it can be deduced that the GM and SOL muscles begin to play an important role towards the end of the first year of life, i.e., when the infant begins to be able to stand and take their first steps independently. GM and SOL control respectively hip flexion and dorsiflexion during standing. The GM is certainly involved even within the first year for precursory locomotor movements such as supine kicking, dependent/independent crawling and scooting, or even during phases of assisted locomotion while holding on to objects or caregivers (Thelen and Fisher, 1982; Thelen et al., 1984; Bly, 1994; Adolph et al., 1998). On the contrary, we are not aware that the SOL (with the plantar flexion movement) plays any relevant role among the precursory locomotor movements. However, it is reasonable to think that GM and SOL begin to make a significant contribution only when external supports for locomotion disappear, and even more so when a mature and efficient bipedal locomotion is acquired around the age of 6.

Since all the entheses respond directly to the biomechanical stimuli imparted by muscle activity we believe it is very important to take the locomotor development into account as a potential etiological agent of any entheseal modifications in subadults.

2. Materials and Methods

In this work we examine the morphometric variability of the femoral insertion of the *gluteus maximus* muscle (GM) and tibial origin of the *soleus* muscle (SOL). Both entheses are fibrous (Havelková and Villotte, 2007; Villotte, 2009; Mann and Hunt, 2012, p. 204; Weiss, 2015; Milella et al., 2020; Villotte and Santos, 2022. entheses).

The sample consists of 119 skeletons of juvenile individuals aged from birth to 30 years (Table 1) belonging to the Documented Human Skeletal Collection of the "Certosa" Cemetry of Bologna (Italy), for which the personal data are known from the cemeterial records (Belcastro et al., 2017, 2022). A subsample of young adults was included in order to observe the morphological variation of the entheses with respect to the last stages of skeletal maturation. Only well-preserved individuals were included in this research, discarding all those where it was impossible to evaluate at least one enthesis on a femur or tibia (i.e., due to taphonomic alterations). Furthermore, the enthesis was considered recordable if at least 50% of its surface was not damaged. Individuals whose femurs or tibiae showed evidence of pathologic conditions (e.g., presence of abundant woven bone, deformations of the diaphysis) were also discarded. The individuals analyzed in this study were divided into 7 age classes (Table 1), where the first two age classes were designated considering the information present in the literature about the early stages of acquiring bipedal gait:

- **Age class 1 (<1 years)**: bipedal locomotion is absent (Thelen and Fisher, 1982; Thelen et al., 1984; Bly, 1994; Adolph et al., 1998).
- **Age class 2 (1-5.9 years)**: bipedal locomotion is present but still immature (toddling). This is therefore a long transitory phase that goes from a rudimental and still dependent locomotion to a mature gait (McGraw, 1940; Forssberg, 1985; Adolph et al., 2003; Hallemans et al., 2003, 2004; Ivanenko et al., 2004; Hallemans et al., 2006a, b; Cowgill et al., 2010; Zeininger et al., 2018; Swan et al., 2020; Pietrobelli et al., 2022a).
- **Age class 3 (6-10.9 years), 4 (11-15.9 years), 5 (16-20.9 years), 6 (21-25.9 years), 7 (26-30 years)**: even though from the age of 6 a bipedal gait is already completely acquired, the remaining individuals have also been divided into quinquennial classes, (except for the last one which covers 4 years) to identify any possible morphological changes in entheses in relation to bone lengthening (classes 3-5) and entheseal "settlement" once the definitive stature has been reached (classes 6-7).

We examined juvenile femurs and tibiae without considering the age *a priori*. The variation observed at the GM was subdivided into 3 morphological classes, whereas variation at the SOL was subdivided into 4 morphological classes, as described in Table 2 and depicted in Figures 1-7. At each morphological class we arbitrarily assigned a number that is not in a predefined order. The assessment of ECs on GM and SOL in juvenile individuals was therefore performed following a new descriptive and photographic standard we created for this purpose (Table 2; Figures 1-7). For each morphological class, photographs of four entheses belonging to four different individuals were provided to better illustrate the variability within the single morphological classes (Figures 1-7). The entheses which were completely covered by *mineralized tissue formations*, in particular characterized by *diffuse cortical irregularities* and *longitudinal protrusions* (typical features of adult individuals) have been assessed with Mariotti et al. (2007) method for entheseal robusticity.

We proceeded taking the linear dimensions of the entheses with a digital sliding caliper (resolution: 0.001 mm):

- The **entheseal length** was taken by measuring the distance between the most proximal and most distal extremities, following the longitudinal axis of the enthesis, regardless of its relative orientation to the bone length. In the case of GM, a possible third trochanter must be included in the measurement, as part of the enthesis. Both extremities must be clearly visible, otherwise the measurement must be considered non-recordable.

- The **entheseal width** was measured at maximum width, therefore according to the transversal axis of the enthesis. Regarding the GM, it is essential that the proximal half of the enthesis is intact, as in this area the gluteal tuberosity is very often wider and more evident. If not, the width must be considered non-recordable. Concerning the SOL, at least the 50% of the enthesis must be intact, regardless of whether it is proximal or distal, as the enthesis does not appear to have significant variations in width along its attachment.

The stage of development of femurs and tibiae was assessed by determining of the degree of epiphyseal closure and bone size. The degree of epiphyseal closure was assessed following the Belcastro et al. (2019) method, which provides a five-degree assessment standard. For statistical convenience, the different degrees of closure of the epiphyses evaluated with this method were reduced to three: 0 corresponds to not fused (equivalent to grade 0), 1 corresponds to partially fused (equivalent to grades 1 and 2) and 2 corresponds to totally merged (equivalent to grades 3 and 4). This adaptation was then extended to the whole bones to assign an overall assessment of its state of maturation: in grade 0 none of the epiphyses are fused, in grade 1 at least one epiphysis is at closure stage 1 or 2, and in grade 2 all bone epiphyses must be fully fused (grade 3 and 4).

Linear measurements of maximum length and transverse diameter at midshaft were taken following the protocols provided by Martin and Saller (1957). Immature bones were instead measured according to Fazekas and Kósa's (1978) protocol. The measurements were considered non-recordable if the cortical bone at the landmarks was damaged.

All statistical analyses were performed in R v.4.2.2. To test the validity of this method to morphometrically assess the GM and SOL entheses, intra- and inter-observer errors were evaluated calculating the Cohen kappa coefficient (κ – Cohen, 1960, 1968) and the accuracy for qualitative variables (i.e., the morphological standards), while the intraclass correlation coefficient (ICC – Fisher, 1954) was opted for the quantitative variables (i.e., all the linear entheseal measurements). The author who executed the inter-observer error had no previous experience on the study of ECs of GM and SOL in juvenile individuals.

Chi-squared tests (X^2) (Pearson, 1900) were performed to test differences in sex and age distribution within the sample and a t-test (Student, 1908) was calculated to evaluate a possible asymmetry between the left and the right side. Descriptive statistics (mean, standard deviation, median, minimum and maximum values) were calculated for each measurement and grouped by age class and sex. The distribution of the morphological classes of GM and SOL by age and sex was represented through boxplots. Normality distribution was assessed with a Shapiro-Wilk normality test (Shapiro and Wilk, 1965). Fisher's exact tests of independence (Fisher, 1934) were calculated to study the distribution of the morphological classes of entheses by sex, by age classes and by sex within the single age classes. Wilcoxon rank-sum tests (Wilcoxon, 1945) were performed to analyze the linear measurements in relation to sex within the age classes. The data were also investigated for possible correlations performing Spearman's tests (Spearman, 1904) between the morphological classes of the entheses and age, linear measurements and epiphyseal closure degree; linear regression models have also been developed for these same variables. The data were finally analyzed performing a Factor Analysis of Mixed Data (i.e., FAMD) using the "FactoMineR" (Lê et al., 2008) and "factoextra" (Kassambara and Mundt, 2020) packages. Specifically, the following variables were included in the FAMD: sex, age, age classes, entheseal morphological classes, linear measurements of the bones and entheses and degree of epiphyseal closure. For this purpose, missing data were replaced with each variable's median value for linear measurements, calculated for each age class and sex.

3. Results

No significant differences were found in the distribution of the sexes by age ($X^2 = 59$; *p*-value >0.05), but differences were detected in the distribution of individuals among the age classes ($X^2 = 82.6$; *p*-value <0.0001). In fact, age class 1 is largely the most represented (especially by males), while age classes 3, 4 and 7 are the least represented. In age class 4 the females are totally absent (Table 1). No differences were found between left and right limb, therefore all the following statistical analyzes were performed only on the left limb. Since not all variables followed a normal distribution or were homoscedastic, nonparametric tests were chosen for the univariate and bivariate statistical analyzes.

The results of the intra- and inter-observer errors are shown in Table 3. The intra-observer results show a high reliability, both concerning the morphological standards and the linear entheseal measurements. The inter-observer results, instead, show very reliable results concerning SOL_morph and all the linear entheseal measurements of GM, while a poorer but still fair/moderate reliability (Landis and Koch, 1977; Koo and Li, 2016) resulted regarding GM_morph, SOL_length and SOL_width.

The most represented morphological classes of GM are GM1, GM2a and GM2b, with a way larger male contribution in class GM2a; regarding the SOL, the most represented morphological class is SOL3 (Table 4). For both GM and SOL, statistically significant differences were only found among age classes. Within age classes significant differences between sexes emerged only in GM in age class 1 (Table 4). Figure 8 shows for both sexes that as the age increases, morphological classes

GM2a, GM2b, GM1 and GM3 follow one another almost without overlapping. A similar pattern can be seen for SOL, where SOL1+SOL2, SOL3 and SOL4 seem to follow one another, even though there does not appear to be a clear separation between SOL1 and SOL2.

Table 5 and Table S1 (i.e., the extended version of Table 5) show the descriptive statistics for linear measurements of bones and entheses by sex and age classes and the results of the Wilcoxon rank-sum test performed by sex within the age classes for each continuous variable; the results of the age classes 3, 4 and 7 and the result of the entheseal length of SOL (SOL_length) in class 1 were not reported due to the small number of observations. By and large females show comparable measurements to males during growth, except for the bone diameters in age class 1 (Femoral_diameter and Tibial_diameter). A more marked sexual dimorphism begins to appear from age class 5. In general, all measurements tend to increase with age.

Table 6 shows the results of the Spearman correlation and linear regression performed between the entheseal morphological classes and age and other variables inherently correlated with age (linear measurements of bones and entheses and epiphyseal closure), both with the distinction between the sexes and together. To perform correlation and linear regressions, it was necessary to convert the morphological classes into ranks. Since the descriptive statistics relating to the morphological classes of GM, more specifically in Figure 8, showed a clear sequence in relation to the age of morphologies GM2a, GM2b, GM1, GM3 and Mariotti subclasses, it was preferred to assign the ranks consistently with this pattern. Regarding the morphological classes of SOL, the rank conversion was performed following the original sequence (SOL1, SOL2, SOL3, SOL4, Mariotti subclasses), as it did not show big discrepancies compared to the pattern shown in the Figure 8. In all the cases, all the considered variables resulted strongly and positively correlated with the morphological classes assigned to the two entheses. Most of the linear regressions show a good predictive power ($r^2 > 0.5$), except for all the linear measurements of tibia and SOL.

Two FAMDs were calculated, one for the GM and all the variables regarding the femur and one for SOL and all the variables regarding the tibia (Figures 9 and S1). In the FAMD calculated for GM morphological classes and related variables, Dim1 explains the 34% of the variance of the dataset, while Dim2 explains the 9% (Figure 9a, b; Figures S1a and S2a). In the FAMD for SOL morphological classes and related variables, instead, Dim1 explains the 37.5% of the variance of the dataset, while Dim2 explains the 9.2% (Figure 9c, d; Figures S1b and S2d). In both cases, Dim1 is mostly driven by age classes, age, all linear measurements, degree of epiphyseal closure and morphological classes (Figure S2b, e); age classes, morphological classes and the degree of epiphyseal closure highly contribute to Dim 2 too (Figure S2c, f). In both cases sex contributed very little (Figures S1a, b and S2b, c, e, f). As far as the GM and femoral variables are concerned (Figures

9a, b and S1a), Dim 1 clearly separates GM2 and GM3+Mariotti subclasses while GM1 encompasses almost all the variability along Dim1, but only considering its confidence interval. A pattern is thus visible (especially by observing the points), which sees a succession among the morphological classes GM2a, GM2b, GM1 and GM3. Dim2 explains the separation between GM1+GM2 and Mariotti subclasses, while GM3 overlaps with Mariotti for higher values and with GM1+GM2 for lower values of Dim2 (Figure 9a). The age classes follow the same pattern, where age classes 1, 2, 3, 4 and 5 plot close to morphologies GM2a, GM2b and GM1, while age classes 6 and 7 are closer to GM3 and the Mariotti subclasses (Figure 9a). Figure 9b shows a complete separation along Dim1 between the individuals who present unfused femoral epiphyses and who present a partial or total state of closure. Morphological classes GM2a and GM2b are strongly associated to unfused femoral epiphyses, GM1 is associated to both unfused and partially/totally fused epiphyses, GM3 is associated to both partially and totally fused epiphyses, and Mariotti subclasses are all associated to totally fused epiphyses. Regarding the SOL and tibial variables (Figure 9c, d; S1b), the morphological classes SOL1+SOL2, SOL3 and SOL4 separate from one another along Dim1, while the separation among SOL4 and the Mariotti subclasses is better explained by Dim 2, although they are still largely overlapped, especially in the negative values of Dim2 (Figure 9d). The confidence intervals of SOL1 and SOL2 do not separate neither along Dim1 nor along Dim2, resulting largely overlapped (Figure 9c); furthermore, SOL1 and SOL2 morphologies fall entirely within the confidence interval of SOL3 (for more negative values), however, the overlap between the points is minimal. The age classes follow the same pattern, where age classes 1, 2, and 5 plot closer to morphologies SOL1, SOL2, SOL3 and SOL4, while age classes 6 and 7 result closer to the Mariotti subclasses (Figure 9c). Figure 9d shows a complete separation along Dim1 between the individuals who present unfused tibial epiphyses and who present a partial or total state of closure. Morphological classes SOL1, SOL2 and SOL3 are strongly associated to unfused femoral epiphyses, while class SOL4 and Mariotti subclasses are associated to partially and totally fused epiphyses. The packages FactoMineR and factoextra excluded the age classes 3 and 4 from the calculation of this FAMD because some variables were not represented in these age classes (i.e., SOL_length in both age classes 3 and 4, SOL_width as regards the females of age class 4).

4. Discussion

Our work sheds light on the variability of ECs during growth highlighting the influence of age, sex and locomotor development.

The results concerning the calculation of the errors (Table 3) showed an overall lower agreement on the inter-observer error, especially on the morphological standard of GM (GM_morph), entheseal length of SOL (SOL_length) and width (SOL_width). As far as concerns GM_morph, the disagreement was almost entirely caused by a difficulty in recognizing the GM1 morphology, specifically, the second observer tended to recognize as GM3 the entheses that the first observer, creator of the standard, recognized as GM1. The discrepancy observed for SOL_length and SOL_width is likely due to the fact that this enthesis is often discontinuous and not well-defined, especially in its proximal extremity. The potential difficulty in identifying clear boundaries in entheses has already been raised in the past (Zumwalt, 2005), however, it was not an obstacle to the research as the most uncertain measures were removed from the analysis.

The morphological variability observed on entheses is continuous, it is self-evident that it is very difficult to divide it into discrete categories and therefore to grasp recurring characteristics. fssStudies on enthesis are generally affected by the experience of the observer (Wilczak et al., 2017),however, the protocol here proposed has the advantage of being easily usable, with acceptable levels of repeatability, and of allowing the evaluation of numerous samples without the need of expensive equipment.

Remarkable **sex differences** emerged neither in the univariate nor in the multivariate statistics (Table 4; Figure S1a, b). The distribution of morphological classes of both GM and SOL do not differ between the sexes, except for a slightly significant difference within age class 1 in GM (Table 4), probably related to the imbalance of the *sex ratio* present in this age class: firstly, because there are way more males than females (Table 1), secondly, because the youngest individuals of age class 1 are male, while the oldest are mostly female (10 females *vs* 25 males in the first 6 months, and 10 females *vs* 3 males in the last 6 months). It is likely that this imbalance is also responsible for the significance that emerged in the same age class as regards the transverse diameter at midshaft of the femur (Femoral_diameter) and tibia (Tibial_diameter), which sees higher dimensions in females rather than males (Tables 5 and S1). Apart from the differences just mentioned, we did not observe significant sex differences in measurements in the first three age classes (i.e., from birth to 10.9 years of age), contrary to what reported in literature for other metric variables (e.g., Malina and Johnston, 1967; Humphrey, 1998; Stull and Godde, 2012; Stull et al., 2017; Luna et al., 2017; Marino et al., 2020). The present study also disagrees with Gonen Aydin et al. (2021), who observed differences between sexes in the gait cycle pattern.

Fisher's exact test of independence (Table 4), Spearman correlation tests and linear regressions (Table 6) and the FAMDs (Figure 9 and S2) reveal the significant role of **age** in explaining variation among the morphological classes of both GM and SOL. Indeed, several studies conducted on adults highlighted a strong relationship between entheseal morphological features and age (Hawkey and Merbs, 1995; Peterson, 1998; Robb, 1998; Eshed et al., 2004; Mariotti et al., 2007;

Alves Cardoso and Henderson, 2010; Milella et al., 2012). This is immediately evident in the descriptive statistics (Figure 8), where the different morphologies follow one another in order of age and characterize well-defined age intervals, especially as regards the GM morphological classes. This pattern and the close relationship with age tends to be less clear considering the Mariotti subclasses (we remind that Mariotti and colleagues' assessment method is applicable on adult individuals only, in this case on long bones with fully closed epiphyses). The FAMD divided by morphological class of the GM (Figure 9a) shows a pattern that sees a distancing between the new morphological classes (i.e., GM2a, GM2b, GM1 and GM3) along Dim1, where age and related variables play a predominant role (Figure S2b), despite a partial overlapping of the confidence intervals. A similar pattern can be seen in the FAMD divided by the morphological classes of the SOL (Figure 9c): the new morphological classes (i.e., SOL1, SOL2, SOL3 and SOL4) result divided along Dim1, with the exception, however, of classes SOL1 and SOL2, whose centroids are very close to each other. On the other hand, for both GM and SOL, the variability of individuals associated with the Mariotti subclasses is best explained by Dim2, where the linear dimensions of bones and entheses play a secondary role (Figure S2c, f), as growth has ceased. Furthermore, the confidence intervals of the single Mariotti subclasses do not separate considerably: this result is not surprising, as there were very few individuals with an enthesis characterized by a complete *mineralized tissue formation* (and therefore detectable with the method developed on adult samples by Mariotti et al., 2007), moreover, 5 morphological subclasses were considered, which are a lot compared to the few individuals.

As regards the relationships between entheseal morphology and **locomotor** milestones, we here consider the EC patterns observable within the first two age classes, as the child acquires a mature locomotor behavior by the age of six (i.e., by the end of age class 2) with the correction of the *genu varum* (Tardieu and Trinkaus, 1994; Swan et al., 2020). For the GM, the GM2a morphology seems to uniquely characterize age class 1, while morphology GM2b characterizes age classes 1 and 2, but with a greater frequency in age class 2. This morphological switch may reflect a locomotor pattern, in fact, just at the end of the first year of life (i.e., age class 1) the infant begins to take their first steps independently (Bly, 1994); therefore, we hypothesize that this new stimulus may represent the cause of this morphological change. Until the age of six, toddlers present a poorly accentuated bicondylar angle of the femur, which causes poor medio-lateral control during locomotion (Tardieu and Trinkaus, 1994; Swan et al., 2020). This skeletal feature causes a "waddling" gait (Cowgill et al., 2010) which we suppose could affect the GM entheseal morphology in this phase. The hypothesis that morphology GM2b may be determined by an immature locomotor behavior is supported by the fact that from age class 3, when the child has fully acquired a complete bipedal locomotion, morphology GM2b disappears, leaving room for morphology GM1 only, characterized by a fine porosity and a much smoother surface. The overlap between GM2a and GM2b in class 1 and between GM2b and GM1 can reflect variability among children in the maturation of their locomotor skills (Bly, 1994). The close relationship between gait biomechanics and age here proposed is also supported by Froehle et al. (2013) and Liu et al. (2022).

The relationship between the morphology of the entheses and locomotor milestones is not clear for SOL instead: age class 1 is characterized by morphology SOL1, SOL2, but above all by SOL3, which is present up to age class 5 (Table 4). Probably these morphologies are not associated to a particular locomotor pattern. One reason that can explain this big difference between the two entheses is that the stimulus imparted from the two entheses on the bones can differ for several reasons. Firstly, the SOL enthesis is an origin, moreover, shared with another bone (i.e., the fibula); on the other hand, the GM enthesis is an insertion, which consequently has to bear a much greater effort since it is located on the bone that performs the movement. Firstly, the SOL enthesis serves as an origin (with another end originating from the fibula). In contrast, the GM enthesis functions as an insertion and is therefore subject to a significantly greater effort due to its location on the bone responsible for the movement. This anatomo-functional difference could also explain why the insertion of the GM on the femur is always visible and much more defined than the tibial origin of the SOL. Moreover, the GM muscle seems to activate before the SOL muscle during life, in fact, it seems to be already involved in the precursory locomotor movements, while the SOL does not seem to have any noteworthy role before the acquisition of an upright posture (Bly, 1994).

Regarding the relationships between entheseal morphology and **epiphyseal closure,** in both the entheses here analyzed, a single morphology dominates in age class 3 (6-10.9 years of age), which are morphological classes GM1 and SOL3 (Table 4). In the following phases, the entheses seem then to evolve into forms characterized by a *mineralized tissue formation* typical of adults (Villotte et al., 2016). In both entheses, however, this shift from a “juvenile-like” to an “adult-like” morphology does not seem to be sudden, in fact, it goes through a sort of “transitional” phase in which a coexistence of typically adult (raised areas) and juvenile (porotic or furrowed zones) characteristics is observed: these are respectively morphology GM3 (Table 4; Figures 3, 8 and 9a) and morphology SOL4 (Table 4; Figures 7, 8 and 9c). This relevant morphological change, or rather at this point, this maturation process of the enthesis, could be triggered by the closure of the epiphyses, that marks the end of the long bone lengthening and thus the “migration” of the enthesis along the diaphysis (Hoyte and Enlow, 1966; Dörfl, 1980a, 1980b; Hurov, 1986). This hypothesis may be supported by the results of the FAMD divided by the degree of epiphyseal closure (Figures 9b, d). In Figure 9b, relating to the enthesis of the GM, morphology GM3 and the Mariotti subclasses (typical of adults) are strongly associated with individuals who present partially or totally fused epiphyses. GM1 instead appears to be associated with all closure degrees, but more commonly with unfused and partially fused epiphyses, while morphological classes GM2a and GM2b are exclusively associated with unfused epiphyses. Given the observed pattern, considering the close correlation between morphologies and age (Table 6) and the division between morphologies observed in Figure 9a, it can be hypothesized that morphology GM1 remains for a short period when the epiphyses begin to fuse, after which a process of gradual mineralization of the enthesis begins and finally leads to a complete ridge.

The enthesis of SOL shows the same pattern (Figure 9d): the “transitional” morphology SOL4 and the Mariotti subclasses for SOL (typical of adults) are strongly associated with individuals who present at least partially fused tibial epiphyses, in which, therefore, bone lengthening has already ceased. Morphological class SOL3, although associated much more with unfused epiphyses, is also present in several individuals with partially fused ones, while morphological classes SOL1 and SOL2 are only associated with unfused epiphyses. The same conclusions drawn for the GM can reasonably be applied on the SOL as well, so considering the close correlation between morphologies and age (Table 6) and the division between morphologies observed in Figure 9c, it can be hypothesized that morphology SOL3 remains for a short period when the epiphyses begin to fuse, after which a process of gradual mineralization of the enthesis begins, finally leading to a complete ridge.

These transformations observed in GM and SOL entheses are attested by the possible presence of woven bone in the “transitional” morphologies GM3 and SOL4 (Table 2, Figures 3 and 7), which may be an indicator of ongoing mineralization (White et al., 2012; Cunningham et al., 2016, pp: 26–29, 34–35).

To sum up, we saw a transformation from a very irregular appearance typical of subadults to a *mineralized tissue formation* in variable degrees of expression (Mariotti et al., 2007). The porotic or furrowed surface of juvenile entheses could therefore be symptoms of a strong bone remodeling due to the migratory process, as Hoyte and Enlow (1966), Dörfl (1980a, 1980b) and Hurov (1986) proposed, which prevents the mineralization of the bone-tendon interface.

5. Conclusions

The present work sheds light on aspects never explored before, providing new important insights into the variability of ECs in modern juvenile individuals. In particular, we gathered more consistent data than before (cf. Belcastro et al., 2020) on the modern juvenile morphological variability. It would be interesting to enlarge the small sample of Neanderthal adult and juvenile entheses to perform more consistent comparisons between the intrapopulation variability of these different human populations.

Through the application of our morphometric recording standard for modern juvenile individuals, we highlight a very clear relationship between the morphometric changes affecting the entheses of GM and SOL muscles and age. For the GM, also a relationship between the morphological ECs and locomotor milestones seems to be observed. Another interesting perspective of this study is the possibility of using these features in subadult-young adult age estimation, with possible applications in bioarcheological and forensic fields. In fact, these methods would permit to estimate the age of juvenile individuals, even from fragmented bones, provided that the enthesis is preserved.

A future goal will certainly be to test our protocol on other documented juvenile skeletal collections, especially enlarging the sample in less represented age classes in this study, in order to deepen the understanding of the relationship between entheseal morphometric changes and development, also in an evolutive perspective.

Author contributions

Davide Mameli: conceptualization; methodology; validation; formal analysis; investigation; writing - original draft; writing - review and editing. **Annalisa Pietrobelli**: conceptualization; validation; formal analysis; writing - review and editing. **Rita Sorrentino**: writing - review and editing. **Teresa Nicolosi**: writing - review and editing. **Valentina Mariotti**: conceptualization; supervision; writing - review and editing. **Maria Giovanna Belcastro**: conceptualization; resources; supervision; project administration; writing - review and editing.

References

Adolph, K. E., Vereijken, B., & Denny, M. A. (1998). Learning to Crawl. *Child Development,69*, 1299–1312. https://doi.org/10.1111/j.1467-8624.1998.tb06213.x

Adolph, K. E., Vereijken, B., & Shrout, P. E. (2003). What Changes in Infant Walking and Why. *Child Development*, *74*, 475–497. https://doi.org/10.1111/1467-8624.7402011

Alves Cardoso, F. & Henderson C. Y. (2010). Enthesopathy Formation in the Humerus: Data from Known Age-at-Death and Known Occupation Skeletal Collections. *American Journal of Physical Anthropology*, *141*, 550–560. https://doi.org/10.1002/ajpa.21171

Belcastro, M. G., Bonfiglioli, B., Pedrosi, M. E., Zuppello, M., Tanganelli, V. & Mariotti, V. (2017). The History and Composition of the Identified Human Skeletal Collection of the Certosa Cemetery (Bologna, Italy, 19th–20th Century). *International Journal of Osteoarcheology*, *27*, 912–925. https://doi.org/10.1002/oa.2605

Belcastro, M.G., & Mariotti, V. (2017). A muscular imprint on the anterolateral surface of the proximal femurs of the Krapina Neandertal collection. *American Journal of Physical Anthropology*, *162*, 583–588. https://doi.org/10.1002/ajpa.23140

Belcastro, M. G., Mariotti, V., Facchini, F. & Bonfiglioli, B. (2006). Musculoskeletal Stress and Adult Age Markers in the Krapina Hominid Collection: The Study of Femora 213 *Fe.1* and 214 *Fe.2*. *Periodicum Biologorum, 108,* 319–329. https://www.scopus.com/inward/record.uri?eid=2-s2.0-33746446789&partnerID=40&md5=7ecd578f3f5652cecbba6f9158e81e36

Belcastro, M. G., Mariotti, V., Pietrobelli, A., Sorrentino, R., García-Tabernero, A., Estalrrich, A., & Rosas, A. (2020). The study of the lower limb entheses in the Neanderthal sample from El Sidrón (Asturias, Spain): How much musculoskeletal variability did Neanderthals accumulate? *Journal of Human Evolution, 141*, 102746. https://doi.org/10.1016/j.jhevol.2020.102746

Belcastro M. G., Pietrobelli A., Nicolosi T., Milella M. & Mariotti V. (2022). Scientific and Ethical Aspects of Identified Skeletal Series: The Case of the Documented Human Osteological Collections of the University of Bologna (Northern Italy). *Forensic Sciences*, *2*(2), 349–361. https://doi.org/10.3390/forensicsci2020025

Belcastro, M. G., Pietrobelli, A., Rastelli, E., Iannuzzi, V., Toselli, S. & Mariotti, V. (2019). Variations in epiphyseal fusion and persistence of the epiphyseal line in the appendicular skeleton of two identified modern (19th–20th c.) adult Portuguese and Italian samples. *American Journal of Physical Anthropology, 169*, 448–463. https://doi.org/10.1002/ajpa.23839

Benjamin, M., Kumai, T., Milz, S., Boszczyk, B.M., Boszczyk, A.A., & Ralphs, J.R. (2002). The skeletal attachment of tendons – tendon 'entheses'. *Comparative Biochemistry and Physiology Part A: Molecular & Integrative Physiology*, *133*(4), 931–45. https://doi.org/10.1016/S1095-6433(02)00138-1

Bly, L. (1994). *Motor skills acquisition in the first year: An illustrated guide to normal development*. Therapy Skill Builders.

Cohen, J. (1960). A coefficient of agreement for nominal scales. *Educational and Psychological Measurement*, *20*, 37–46. https://doi.org/10.1177/001316446002000104

Cohen, J. (1968). Weighted kappa: nominal scale agreement with provision for scaled disagreement or partial credit. *Psychological Bulletin*, *70*, 213–220. https://doi.org/10.1037/h0026256

Colombo, A., Stephens, N. B., Tsegai, Z. J., Bettuzzi, M., Morigi, M. P., Belcastro, M. G., & Hublin, J.-J. (2019). Trabecular Analysis of the Distal Radial Metaphysis during the Acquisition of Crawling and Bipedal Walking in Childhood: A Preliminary Study. *Bulletins et Memoires de la Société d'Anthropologie de Paris, 31*(1-2), 43–51.

Cowgill, L. W., Warrener, A., Pontzer, H., & Ocobock, C. (2010). Waddling and Toddling: The Biomechanical Effects of an Immature Gait. *American Journal of Physical Anthropology, 143*, 52–61. https://doi.org/10.1002/ajpa.21289

Cunha, E. & Umbelino, C. (1995). What can bones tell about labour and occupation: the analysis of skeletal markers of occupational stress in the Identified Skeletal Collection of the Anthropological Museum of the University of Coimbra (preliminary results). *Antropologia Portuguesa*, *13*, 49–68.

Cunningham, C., Scheuer, J. L., & Black, S. M. (2016). *Developmental Juvenile Osteology* (2nd ed.). Elsevier Academic Press.

Dörfl, J. (1980a). Migration of tendinous insertions. I. Cause and mechanism. *Journal of Anatomy, 131*, 179–195.

Dörfl, J. (1980b). Migration of tendinous insertions. II. Experimental modifications. *Journal of Anatomy*, *131*, 229–237.

Dutour, O. (1986). Enthesopathies (Lesions of Muscular Insertions) as Indicators of the Activities of Neolithic Saharan Populations. *American Journal of Physical Anthropology, 71*, 221–224. https://doi.org/10.1002/ajpa.1330710209

Eshed, V., Gopher, A., Galili, E. & Hershkovitz, I. (2004). Musculoskeletal Stress Markers in Natufian Hunter-Gatherers and Neolithic Farmers in the Levant: The Upper Limb. *American Journal of Physical Anthropology, 123*, 303–315. https://doi.org/10.1002/ajpa.10312

Fazekas, I. G. & Kósa, F. (1978). *Forensic Fetal Osteology*. Budapest: Akadémiai Kiadó.

Figus, C., Stephens, N. B., Sorrentino, R., Bortolini, E., Arrighi, S., Higgins, O. A., Lugli, F., Marciani, G., Oxilia, G., Romandini, M., Silvestrini, S., Baruffaldi, F., Belcastro, M. G., Bernardini, F., Festa, A., Hajdu, T., Mateovics-László, O., Pap, I., Szeniczey, T., Tuniz, C., Ryan, T. M., & Benazzi, S. (2023). Morphologies in-between: The impact of the first steps on the human talus. *The Anatomical Record, 306*(1), 124–142. https://doi.org/10.1002/ar.25010

Figus, C., Stephens, N. B., Sorrentino, R., Bortolini, E., Arrighi, S., Lugli, F., Marciani, G., Oxilia, G., Romandini, M., Silvestrini, S., Baruffaldi, F., Belcastro, M. G., Bernardini, F., Erjavec, I., Festa, A., Hajdu, T., Mateovics-László, O., Novak, M., Pap, I., Szeniczey, T., Tuniz, C., Ryan, T. M., & Benazzi, S. (2022). Human talar ontogeny: Insights from morphological and trabecular changes during postnatal growth. *American Journal of Biological Anthropology, 179*(2), 211–228. https://doi.org/10.1002/ajpa.24596

Fisher, R. A. (1934). *Statistical methods for research workers* (5th ed.). Oliver and Boyd: Edinburgh.

Fisher, R. A. (1954). *Statistical methods for research workers* (12th ed.). Oliver and Boyd: Edinburgh.

Forssberg, H. (1985). Ontogeny of human locomotor control I. infant stepping, supported locomotion and transition to independent locomotion. *Experimental Brain Research*, *57*, 480–493. https://doi.org/10.1007/BF00237835

Froehle, A. W., Nahhas, R. W., Sherwood, R. J., & Duren, D. L. (2013). Age-related changes in spatiotemporal characteristics of gait accompany ongoing lower limb linear growth in late childhood and early adolescence. *Gait & posture*, *38*(1), 14–19. https://doi.org/10.1016/j.gaitpost.2012.10.005

Gonen Aydin, C., Hale Hekim, H., Ucpinar, H., Oztas, D., & Avni Bayhan, I. (2021). Gender differences between the three dimensional gait analysis data of young athletes. *Annals of Medical Research*, *27*(7), 1949–1955. https://annalsmedres.org/index.php/aomr/article/view/857

Hallemans, A., Aerts, P., Otten, B., De Deyn, P. P., & De Clercq, D. (2004). Mechanical energy in toddler gait. A trade-off between economy and stability? *Journal of Experimental Biology*, *207*, 2417–2431. https://doi.org/10.1242/jeb.01040

Hallemans, A., D'Août, K., De Clercq, D., & Aerts, P. (2003). Pressure distribution patterns under the feet of new walkers: The first two months of independent walking. *Foot & Ankle International*, *24*, 444–453. https://doi.org/10.1177/107110070302400513

Hallemans, A., De Clercq, D., & Aerts, P. (2006). Changes in 3D joint dynamics during the first 5 months after the onset of independent walking: A longitudinal follow-up study. *Gait & Posture*, *24*, 270–279. https://doi.org/10.1016/j.gaitpost.2005.10.003

Hallemans, A., De Clercq, D., Dongen, S. V., & Aerts, P. (2006). Changes in foot-function parameters during the first 5 months after the onset of independent walking: A longitudinal follow-up study. *Gait & Posture*, *23*, 142–148. https://doi.org/10.1016/j.gaitpost.2005.01.003

Havelková, P. & Villotte, S. (2007). Enthesopathies: Test of reproducibility of the new scoring system based on current medical data. *Slovenská antropológia*, *10*(1), 51–57.

Hawkey, D. E., & Merbs, C. F. (1995). Activity-induced Musculoskeletal Stress Markers (MSM) and Subsistence Strategy Changes among Ancient Hudson Bay Eskimos. *International Journal of Osteoarchaeology*, *5*, 324–338. https://doi.org/10.1002/oa.1390050403

Henderson, C. Y., Mariotti, V., Pany-Kucera, D., Villotte, S., & Wilczak, C. (2016). The New 'Coimbra Method': A Biologically Appropriate Method for Recording Specific Features of Fibrocartilaginous Entheseal Changes. *International Journal of Osteoarchaeology*, *26*, 925–932. https://doi.org/10.1002/oa.2477

Henderson C. Y., Wilczak C. A., & Mariotti V. (2017). Commentary: An Update to the new Coimbra Method for Recording Entheseal Changes. *International Journal of Osteoarchaeology*, *27*, 522-523. https://doi.org/10.1002/oa.2548

Hoyte, D. A. N. & Enlow, D. H. (1966), Wolff's law and the problem of muscle attachment on resorptive surfaces of bone. *American Journal of Physical Anthropology*, *24*, 205–213. https://doi.org/10.1002/ajpa.1330240209

Humphrey, L. T. (1998). Patterns of growth in the modern human skeleton. *American Journal of Physical Anthropology*, *105*, 57–72. https://doi.org/10.1002/(SICI)1096-8644(199801)105:1<57::AID-AJPA6>3.0.CO;2-A

Hurov, J. R. (1986). Soft-Tissue Bone Interface: How Do Attachments of Muscles, Tendons, and Ligaments Change During Growth? A Light Microscopic Study. *Journal of Morphology*, *189*, 313–325. https://doi.org/10.1002/jmor.1051890309

Ivanenko, Y. P., Dominici, N., Cappellini, G., Dan, B., Cheron, G., & Lacquaniti, F. (2004). Development of pendulum mechanism and kinematic coordination from the first unsupported steps in toddlers. *Journal of Experimental Biology*, *207*, 3797–3810. https://doi.org/10.1242/jeb.01214

Jurmain, R., & Villotte, S. (2010). Terminology. Entheses in medical literature and physical anthropology: a brief review [Online]. Document published online on 4th February following the Workshop in Musculoskeletal Stress Markers (MSM): limitations and achievements in the reconstruction of past activity patterns, University of Coimbra, July 2–3, 2009. Coimbra, CIAS - Centro de Investigação em Antropologia e Saúde. [Consulted on 24th April 2023]. Available from: https://www.uc.pt/en/cia/msm/MSM_terminology3.pdf

Karakostis, F. A. & Harvati, K. (2021). New horizons in reconstructing past human behavior: Introducing the "Tübingen University Validated Entheses-based Reconstruction of Activity" method. *Evolutionary Anthropology*, *30*, 185–198. https://doi.org/10.1002/evan.21892

Karakostis, F.A., Buikstra, J.E., Prevedorou, E., Hannigan, E.M., Hotaling, J., Hotz, G., Liedl, H., Moraitis, K., Siek, T.J., Waltenberger, L., Widrick, K.J., Harvati, K. (2021). New insights into the manual activities of individuals from the Phaleron cemetery (Archaic Athens, Greece). *Journal of Archaeological Science*, *131*, 105415. https://doi.org/10.1016/j.jas.2021.105415

Kassambara, A., & Mundt, F. (2020) Factoextra: Extract and Visualize the Results of Multivariate Data Analyses. R Package Version 1.0.7. https://CRAN.R-project.org/package=factoextra

Kennedy, K. (1998). Markers of Occupational Stress: Conspectus and Prognosis of Research. *International Journal of Osteoarchaeology*, *8*, 305–310. https://doi.org/10.1002/(SICI)1099-1212(1998090)8:5<305::AID-OA444>3.0.CO;2-A

Koo, T. K., & Li, M. Y. (2016). A Guideline of Selecting and Reporting Intraclass Correlation Coefficients for Reliability Research. *Journal of chiropractic medicine*, *15*(2), 155–163. https://doi.org/10.1016/j.jcm.2016.02.012

Landis, J. R., & Koch, G. G. (1977). The Measurement of Observer Agreement for Categorical Data. *Biometrics, 33*(1), 159–174. https://doi.org/10.2307/2529310

Lê, S., Josse, J., & Husson, F. (2008). FactoMineR: An R Package for Multivariate Analysis. *Journal of Statistical Software, 25*(1), 1–18. https://doi.org/10.18637/jss.v025.i01

Liu, W., Mei, Q., Yu, P., Gao, Z., Hu, Q., Fekete, G., István, B., & Yaodong, G. (2022). Biomechanical Characteristics of the Typically Developing Toddler Gait: A Narrative Review. *Children*, *9*(3), 406. http://dx.doi.org/10.3390/children9030406

Luna, L. H., Aranda, C. M., & Santos, A. L. (2017). New method for sex prediction using the human non-adult auricular surface of the ilium in the collection of identified skeletons of the University of Coimbra. *International Journal of Osteoarchaeology*, *27*, 898–911. https://doi.org/10.1002/oa.2604

Malina, R., & Johnston, F. (1967). Relations between bone, muscle, and fat widths in the upper arms and calves of boys and girls studied cross-sectionally at ages 6 to 16 years. *Human Biology*, *39*, 211–223.

Mann, R. W., & Hunt, D. R. (2012). *Photographic Regional Atlas of Bone Disease*. *A Guide to Pathologic and Normal Variation in the Human Skeleton* (3rd ed). Charles C. Thomas Publisher.

Marino, R., Tanganelli, V., Pietrobelli, A., & Belcastro, M. G. (2020). Evaluation of the auricular surface method for subadult sex estimation on Italian modern (19th to 20th century) identified skeletal collections. *American Journal of Physical Anthropology*, *174*, 792–803. https://doi.org/10.1002/ajpa.24146

Mariotti, V. & Belcastro, M. G. (2011). Lower limb entheseal morphology in the Neandertal Krapina population (Croatia, 130 000 BP). *Journal of Human Evolution*, *60*, 694–702. https://doi.org/10.1016/j.jhevol.2010.12.007

Mariotti V., Facchini F., & Belcastro M. G. (2004). Enthesopathies – Proposal of a Standardized Scoring Method and Applications. *Collegium Antropologicum*, *28*(1), 145-159.

Mariotti, V., Facchini, F., & Belcastro, M. G. (2007). The study of entheses: proposal of a standardised scoring method for twenty-three entheses of the postcranial skeleton. *Collegium Antropologicum*, *31*(1), 291–313.

Mariotti, V., Milella, M., & Belcastro, M. G. (2009). Musculoskeletal stress markers (MSM): methodological reflections. In: Workshop in Musculoskeletal Stress Markers (MSM):

Limitations and Achievements in the Reconstruction of Past Activity Patterns. Coimbra, Portugal, July 2-3, 2009. https://www.uc.pt/en/cia/msm/MSM_podium

Martin, R., & Saller, K. (1957). *Lehrbuch der Anthropologie: in systematischer darstellung mit besonderer berücksichtigung der anthropologischen methoden*. Vol. 1. Gustav Fischer Verlag, Stuttgart.

Matyas, J. R., Bodie, D., Andersen, M., & Frank, C. B. (1990). The development morphology of a “periosteal” ligament insertion: Growth and maturation of the tibial insertion of the rabbit medial collateral ligament. *Journal of Orthopaedic Research, 8*, 412–424. https://doi.org/10.1002/jor.1100080313

McGraw, M. B. (1940). Neuromuscular development of the human infant as exemplified in the achievement of erect locomotion. *Journal of Pediatrics, 17*, 747–771. https://doi.org/10.1016/S0022-3476(40)80021-8

Milella, M, Belcastro, MG, Mariotti, V, Nikita, E. Estimation of adult age-at-death from entheseal robusticity: A test using an identified Italian skeletal collection. Am J Phys Anthropol. 2020; 173: 190–199. https://doi.org/10.1002/ajpa.24083

Milella, M., Belcastro, M. G., Zollikofer, C. P. E., & Mariotti, V. (2012). The Effect of Age, Sex, and Physical Activity on Entheseal Morphology in a Contemporary Italian Skeletal Collection. *American Journal of Physical Anthropology, 148*, 379–388. https://doi.org/10.1002/ajpa.22060

Neumann, D. A. (2009). *Kinesiology of the musculoskeletal system: foundations for physical rehabilitation* (2nd ed). Mosby, New York.

Niinimäki, S. (2011). What do Muscle Marker Ruggedness Scores Actually Tell us? *International Journal of Osteoarchaeology, 21*, 292–299. https://doi.org/10.1002/oa.1134

Palmer, J. L. A., Lieverse, A. R. & Waters-Rist, A. L. (2023). A Recording Method for Sixteen Nonadult Muscle Entheses. *Childhood in the Past*. https://doi.org/10.1080/17585716.2023.2275850

Pearson, K. (1900). X. On the criterion that a given system of deviations from the probable in the case of a correlated system of variables is such that it can be reasonably supposed to have arisen from random sampling. *Philosophical Magazine Series 5, 50*(302), 157–175. https://doi.org/10.1080/14786440009463897

Peterson, J. (1998). The Natufian Hunting Conundrum: Spears, Atlatls, or Bows? Musculoskeletal and Armature Evidence. *International Journal of Osteoarchaeology, 8*, 378–389. https://doi.org/10.1002/(SICI)1099-1212(1998090)8:5<378::AID-OA436>3.0.CO;2-I

Pietrobelli, A., Marchi, D., & Belcastro, M. G. (2022a). The relationship between bipedalism and growth: A metric assessment in a documented modern skeletal collection (Certosa Collection, Bologna, Italy). *American Journal of Biological Anthropology*, *177*, 669–689. https://doi.org/10.1002/ajpa.24440

Pietrobelli, A., Sorrentino, R., Durante, S., Marchi, D., Benazzi, S., & Belcastro, M. G. (2022b). Sexual Dimorphism in the Fibular Extremities of Italians and South Africans of Identified Modern Human Skeletal Collections: A Geometric Morphometric Approach. *Biology*, *11*(7), 1079. https://doi.org/10.3390/biology11071079

Pietrobelli, A., Sorrentino, R., Benazzi, S., Belcastro, M. G., & Marchi, D. (2023). Linking the proximal tibiofibular joint to hominid locomotion: A morphometric study of extant species. *American Journal of Biological Anthropology*, 1–20. https://doi.org/10.1002/ajpa.24696

Robb, J. E. (1998). The Interpretation of Skeletal Muscle Sites: A Statistical Approach. *International Journal of Osteoarchaeology*, *8*, 363–377. https://doi.org/10.1002/(SICI)1099-1212(1998090)8:5<363::AID-OA438>3.0.CO;2-K

Shapiro, S., & Wilk, M. (1965). An analysis of variance test for normality (complete samples). *Biometrika*, *52*(3/4), 591–611. https://doi.org/10.1093/biomet/52.3-4.591

Sorrentino, R., Belcastro, M. G., Figus, C., Stephens, N. B., Turley, K., Harcourt-Smith, W., Ryan, T. M., & Benazzi, S. (2020a). Exploring sexual dimorphism of the modern human talus through geometric morphometric methods. *PLoS ONE*, *15*(2), e0229255. https://doi.org/10.1371/journal.pone.0229255

Sorrentino, R., Carlson, K. J., Bortolini, E., Minghetti, C., Feletti, F., Fiorenza, L., Frost, S., Jashashvili, T., Parr, W., Shaw, C., Su, A., Turley, K., Wroe, S., Ryan, T. M., Balcastro, M. G., & Benazzi, S. (2020b). Morphometric analysis of the hominin talus: Evolutionary and functional implications. *Journal of Human Evolution*, *142*, 102747. https://doi.org/10.1016/j.jhevol.2020.102747

Sorrentino, R., Stephens, N. B., Carlson, K. J., Figus, C., Fiorenza, L., Frost, S., Harcourt-Smith, W., Parr, W., Saers, J., Turley, K., Wroe, S., Belcastro, M. G., Ryan, T. M., & Benazzi, S. (2019). The influence of mobility strategy on the modern human talus. *American Journal of Physical Anthropology*, *171*, 456–469. https://doi.org/10.1002/ajpa.23976

Spearman, C. (1904). The Proof and Measurement of Association between Two Things. *The American Journal of Psychology*, *15*(1), 72–101. https://doi.org/10.2307/1412159

Student. (1908). The Probable Error of a Mean. *Biometrika*, *6*, 1–25. https://doi.org/10.1093/biomet/6.1.1

Stull, K. E., & Godde, K. (2012). Sex estimation of infants between birth and one year through discriminant analysis of the Humerus and Femur. *Journal of Forensic Sciences*, *58*, 13–20. https://doi.org/10.1111/j.1556-4029.2012.02286.x

Stull, K. E., L'Abbé, E. N., & Ousley, S. D. (2017). Subadult sex estimation from diaphyseal dimensions. *American Journal of Physical Anthropology*, *163*, 64–74. https://doi.org/10.1002/ajpa.23185

Swan, K. R., Ives, R., Wilson, L. A. B., & Humphrey, L. T. (2020). Ontogenetic changes in femoral cross-sectional geometry during childhood locomotor development. *American Journal of Physical Anthropology*, *173*, 80–95. https://doi.org/10.1002/ajpa.24080

Tardieu, C., & Trinkaus, E. (1994). Early Ontogeny of the Human Femoral Bicondylar Angle. *American Journal of Physical Anthropology*, *95*, 183–195. https://doi.org/10.1002/ajpa.1330950206

Thelen, E., & Fisher, D. M. (1982). Newborn stepping: An explanation for a “disappearing” reflex. *Developmental Psychology*, *18*, 760–775. https://doi.org/10.1037/0012-1649.18.5.760

Thelen, E., Fisher, D. M., & Ridley-Johnson, R. (1984). The Relationship between Physical Growth and a Newborn Reflex. *Infant Behavior and Development*, *7*, 479–493. https://doi.org/10.1016/S0163-6383(84)80007-7

Villotte, S. (2009). *Enthésopathies et activités des hommes préhistoriques Recherche méthodologique et application aux fossiles européens du Paléolithique supérieur et du Mésolithique*. BAR International Series 1992. Archaeopress. https://doi.org/10.30861/9781407305264

Villotte, S., Assis, A., Alves Cardoso, F., Henderson, C. Y., Mariotti, V., Milella, M., Pany-Kucera, D., Speith, N., Wilczak, C. A., & Jurmain, R. (2016). In search of consensus: Terminology for entheseal changes (EC). *International Journal of Paleopathology*, *13*, 49–55. https://doi.org/10.1016/j.ijpp.2016.01.003

Villotte, S., Castex, D., Couallier, V., Dutour, O., Knüsel, C. J., & Henry-Gambier, D. (2010). Enthesopathies as Occupational Stress Markers: Evidence from the Upper Limb. *American Journal of Physical Anthropology*, *142*, 224–234. https://doi.org/10.1002/ajpa.21217

Villotte, S., & Knüsel, C. J. (2013). Understanding Entheseal Changes: Definition and Life Course Changes. *International Journal of Osteoarchaeology*, *23*, 135–146. https://doi.org/10.1002/oa.2289

Villotte, S., & Santos, F. (2023). The effect of age on entheseal changes: A study of modifications at appendicular attachment sites in a large sample of identified human skeletons. *International Journal of Osteoarchaeology*, *33*(3), 389–401. https://doi.org/10.1002/oa.3197

Wei, X., & Messner, K. (1996). The postnatal development of the insertions of the medial collateral ligament in the rat knee. *Anatomy and Embryology*, *193*, 53–59. https://doi.org/10.1007/BF00186833

Weiss, E. (2003). Understanding Muscle Markers: Aggregation and Construct Validity. *American Journal of Physical Anthropology*, *121*(3), 230–240. https://doi.org/10.1002/ajpa.10226

Weiss, E. (2015). Examining Activity Patterns and Biological Confounding Factors: Differences between Fibrocartilaginous and Fibrous Musculoskeletal Stress Markers. *International Journal of Osteoarchaeology*, *25*, 281–288. https://doi.org/10.1002/oa.2290

White, T. D., Black, M. T., & Folkens, P. A. (2012). *Human Osteology* (3rd ed.) Elsevier Academic Press, pp: 35, 36, 40.

Whittle, M. (2006). *An introduction to gait cycle* (4th ed). Butterworth-Heinemann, Edinburgh.

Wilcoxon, F. (1945). Individual Comparisons by Ranking Methods. *Biometrics Bulletin*, *1*(6), 80–83. https://doi.org/10.2307/3001968

Wilczak, C. A., Mariotti, V., Pany-Kucera, D., Villotte, S., & Henderson, C. Y. (2017). Training and interobserver reliability in qualitative scoring of skeletal samples. *Journal of Archaeological Science: Reports*, *11*, 69–79. https://doi.org/10.1016/j.jasrep.2016.11.033

Zeininger, A., Schmitt, D., Jensen, J. L., & Shapiro, L. J. (2018). Ontogenetic changes in foot strike pattern and calcaneal loading during walking in young children. *Gait & Posture*, *59*, 18–22. https://doi.org/10.1016/j.gaitpost.2017.09.027

Zumwalt, A. (2005). A new method for quantifying the complexity of muscle attachment sites. *The Anatomical Record*, *286B*, 21–28. https://doi.org/10.1002/ar.b.20075

Supporting information

Table S1. Descriptive statistical analysis (mean, standard deviation, median and min-max values) for linear measurements of the femur and GM enthesis (left) and tibia and SOL enthesis (right) with the distinction between sex and age class *(Extended version of Table 5, main text)*. All values are expressed in mm.

(The table should be placed here)

Note. Age class 1: <1 year; age class 2: 1-5.9 years; age class 3: 6-10.9 years; age class 4: 11-15.9 years; age class 5: 16-20.9 years; age class 6: 21-25.9 years; age class 7: 26-30 years. -: not available. Abbreviations: F, females; M, males; N, number of individuals; Femoral_length, maximum length of the femur; Femoral_diameter, transverse diameter at midshaft of the femur; GM_length, entheseal length of *gluteus maximus*; GM_width, entheseal width of *gluteus maximus*; Tibial_length, maximum length of the tibia; Tibial_diameter, transverse diameter at midshaft of the tibia; SOL_length, entheseal length of *soleus*; SOL_width, entheseal width of *soleus*. W: Wilcoxon rank-sum test calculated on the linear measurements of the femur and GM enthesis (left) and tibia and SOL enthesis (right) by sex within age classes; *: $p < 0.05$, **: $p < 0.01$, ***: $p < 0.001$ and ****: $p < 0.0001$; NS: nonsignificant result.

Figure S1. FAMDs relating to GM (a) and SOL (b) entheses divided sex.

(The figure should be placed here)

Note: The points indicating the centroids of the ellipses are wider and have a colored outline.

Abbreviations: F, females; M, males. GM_morph (GM1, 2a, 2b, 3 and 1a, 1b, 1c, 2, 3Mariotti), morphological classes of *gluteus maximus*; SOL_morph (SOL1, 2, 3, 4 and 1a, 1b, 1c, 2, 3Mariotti), morphological classes of *soleus*. Femoral_closure and Tibial_closure (0.Fem/0.Tib: unfused epiphyses, 1.Fem/1.Tib: partial state of closure, 2.Fem/2.Tib: total state of closure), degree of epiphyseal closure of the femur and tibia, respectively. Class1, age class 1 (<1 year); Class2, age class 2 (1-5.9 years); Class3, age class 3 (6-10.9 years); Class4, age class 4 (11-15.9 years); Class5, age class 5 (16-20.9 years); Class6, age class 6 (21-25.9 years); Class7, age class 7 (26-30 years).

Figure S2. Scree plots and diagrams of the contributions of the variables to Dimensions 1 and 2 of the FAMD relating to GM (**a**, **b**, **c**) and SOL (**d**, **e**, **f**) entheses.

(The figure should be placed here)

Abbreviations: GM_morph, morphological classes of *gluteus maximus*; SOL_morph, morphological classes of *soleus*; Femoral_length, maximum length of the femur; Femoral_diameter, transverse diameter at midshaft of the femur; GM_length, entheseal length of *gluteus maximus*; GM_width, entheseal width of *gluteus maximus*; Tibial_length, maximum length of the tibia; Tibial_diameter, transverse diameter at midshaft of the tibia; SOL_length, entheseal length of *soleus*; SOL_width, entheseal width of *soleus*; Femoral_closure, degree of epiphyseal closure of the femur; Tibial_closure, degree of epiphyseal closure of the tibia.

Tables

Table 1. Distribution by sex and age of the sample.

Age class	Years	F	M	Total
1	<1	20	28	48
2	1-5.9	13	9	22
3	6-10.9	2	3	5
4	11-15.9	-	4	4
5	16-20.9	7	11	18
6	21-25.9	6	9	15
7	26-30	5	2	7
Total		53	66	**119**

Note. -: not available.
Abbreviations: F, females; M, males.

Table 2. Morphological standard for GM (**top**) and SOL (**bottom**) entheses.

GM_morph[1]	Description
GM1	The enthesis is defined by a diffuse dense *fine porosity* (Figure 1).
GM2	The enthesis is defined by a *furrowed surface* (Figure 2). If the enthesis is mainly characterized (for more than 50% of its surface) by furrows arranged neatly between each other and oriented longitudinally with respect to the length of the diaphysis, assign the morphological subclass **GM2a** (Figure 2, top); if, on the other hand, the enthesis is characterized mainly (for more than 50% of its surface) by regions in which the furrows have a disordered disposition, then assign the subclass **GM2b** (Figure 2, bottom). In cases where a mixed morphology occurs, neatly oriented furrows are usually found proximally, while messily oriented furrows are more commonly found distally.
GM3	The enthesis is characterized by a mixed morphology: the same enthesis shows regions with *diffuse cortical irregularity* and/or a *longitudinal protrusion* and others with a rather smooth surface defined by a *fine porosity* or smooth *furrows*. The *mineralized tissue formations* can generally be found from the proximal border and along the medial border of the enthesis, while the finely porous smooth surface is generally prevalent at the distal and lateral border, thus tracing a proximal-distal pattern. The *mineralized tissue formations* can be covered by a layer of *woven bone*, either continuously or discontinuously (Figure 3).

SOL_morph[2]	Description
SOL1	The enthesis is totally indistinguishable, there is no type of morphological discontinuity between the entheseal area and the surrounding bone (Figure 4).
SOL2	The inferolateral border of the triangular surface covered by the *popliteus* muscle is sharply defined by the soleal line, which separates an area of porous-looking bone (i.e., the triangular "popliteal" surface – Cunningham et al., 2016, pp: 415–416) from the cortical surface distal to it. The enthesis appears only as a line with no width (Figure 5).
SOL3	The enthesis is defined by *furrowed surface* with short and shallow furrows. The furrows may enclose oval-shaped pores (Figure 6).
SOL4	The enthesis is characterized by a mixed morphology: the same enthesis shows regions with *diffuse cortical irregularity* and/or a *longitudinal protrusion* and others with a *finely porous*/*furrowed surface*. The two morphologies coexist on the same enthesis and can appear discontinuously along it, but the *mineralized tissue formations* occur more frequently in the distal portion of the enthesis, while the porotic/furrowed surface proximally, thus tracing a distal-proximal pattern. The *mineralized tissue formations* can be covered by a layer of *woven bone*, either continuously or discontinuously (Figure 7).

Note. If more more than 50% of the enthesal surface is damaged the evaluation must be considered nonrecordable (NR).

[1]: All juvenile GM morphologies can be either on a flat surface or in a fossa; in some cases, especially when the enthesis presents a fossa, the borders of the enthesis can be angled and well evident and should not be confused with a longitudinal protrusion. In GM3 the *mineralized tissue formations* never affect the entire surface of the enthesis, and this distinguishes this morphology from those typical of adults (Mariotti et al., 2007).

[2]: The trace of the SOL enthesis is often discontinuous and there are areas where the trace is totally absent, most often in its proximal half. In younger individuals, the proximal portion of the enthesis can be indistinguishable among the porosity that characterizes the popliteal surface. In these cases, the morphologic assessment must necessarily be performed in its visible portion. In morphological classes SOL2, SOL3 and SOL4 a fossa can be present, which can be constituted by a single or more different sunken areas on the same enthesis.

Abbreviations: GM_morph, morphological classes of *gluteus maximus*; SOL_morph, morphological classes of *soleus*.

Table 3. Intraobserver and interobserver error results.

	Intraobserver error		**Interobserver error**	
Morphological standards	*κ* [a]	*Accuracy*	*κ* [a]	*Accuracy*
GM_morph	0.93	95%	0.21	65%
SOL_morph	0.98	95%	0.90	75%
Linear entheseal measurements	*ICC* [b]		*ICC* [b]	
GM_length	0.98		0.93	
GM_width	0.93		0.81	
SOL_length	0.97		0.55	
SOL_width	0.87		0.53	

Note. [a]: Cohen kappa coefficient. [b]: Intraclass correlation coefficient.
Abbreviations: GM_morph, morphological classes of *gluteus maximus*; SOL_morph, morphological classes of *soleus*; GM_length, entheseal length of *gluteus maximus*; GM_width, entheseal width of *gluteus maximus*; SOL_length, entheseal length of *soleus*; SOL_width, entheseal width of *soleus*.

Table 4. Subdivision of the individuals by the different morphological classes of GM (**top**) and SOL (**bottom**) entheses they have been assigned to, with the distinction between sex and age class.

GM_morph	**Age class 1**		**Age class 2**		**Age class 3**		**Age class 4**		**Age class 5**		**Age class 6**		**Age class 7**		**Total**		
	F	**M**	**F**	**M**	**F**	**M**	**F**	**M**	**F**	**M**	**F**	**M**	**F**	**M**	**F**	**M**	**F+M**
GM1	1	-	5	2	2	3	-	3	4	5	-	3	-	-	12	16	28 (23.5%)
GM2a	12	25	-	-	-	-	-	1	-	-	-	-	-	-	12	26	38 (31.9%)
GM2b	7	3	8	7	-	-	-	-	-	-	-	-	-	-	15	10	25 (21.0%)
GM3	-	-	-	-	-	-	-	-	3	4	2	3	1	-	6	7	13 (10.9%)
1a Mariotti	-	-	-	-	-	-	-	-	-	1	1	-	-	-	1	1	2 (1.7%)
1b Mariotti	-	-	-	-	-	-	-	-	-	-	1	-	1	-	2	-	2 (1.7%)
1c Mariotti	-	-	-	-	-	-	-	-	-	-	2	2	2	-	4	2	6 (5.0%)
2 Mariotti	-	-	-	-	-	-	-	-	-	1	-	-	1	1	1	2	3 (2.5%)
3 Mariotti	-	-	-	-	-	-	-	-	-	-	-	1	-	1	-	2	2 (1.7%)
Total	20	28	13	9	2	3	-	4	7	11	6	9	5	2	**53**	**66**	**119**
F test by sex ^{NS}, by age class ***																	
F test by sex within age classes	*		NS		NS		-		NS		NS		NS				

SOL_morph	**Age class 1**		**Age class 2**		**Age class 3**		**Age class 4**		**Age class 5**		**Age class 6**		**Age class 7**		**Total**		
	F	**M**	**F**	**M**	**F**	**M**	**F**	**M**	**F**	**M**	**F**	**M**	**F**	**M**	**F**	**M**	**F+M**
SOL1	1	5	-	1	-	-	-	-	-	-	-	-	-	-	1	6	7 (5.9%)
SOL2	4	8	-	-	-	-	-	-	-	-	-	-	-	-	4	8	12 (10.1%)
SOL3	15	15	13	8	2	3	-	1	4	2	-	-	-	-	34	29	63 (52.9%)
SOL4	-	-	-	-	-	-	-	3	3	7	3	4	1	-	7	14	21 (17.6%)
1a Mariotti	-	-	-	-	-	-	-	-	-	-	-	-	1	-	1	-	1 (0.8%)
1b Mariotti	-	-	-	-	-	-	-	-	-	-	1	1	-	-	1	1	2 (1.7%)
1c Mariotti	-	-	-	-	-	-	-	-	-	1	2	-	2	-	4	1	5 (4.2%)
2 Mariotti	-	-	-	-	-	-	-	-	-	1	-	4	1	1	1	6	7 (5.9%)
3 Mariotti	-	-	-	-	-	-	-	-	-	-	-	-	-	1	-	1	1 (0.8%)
Total	20	28	13	9	2	3	-	4	7	11	6	9	5	2	**53**	**66**	**119**
F test by sex ^{NS}, by age class ***																	
F test by sex within age classes	NS		NS		NS		-		NS		NS		NS				

Note. Age class 1: <1 year; age class 2: 1-5.9 years; age class 3: 6-10.9 years; age class 4: 11-15.9 years; age class 5: 16-20.9 years; age class 6: 21-25.9 years; age class 7: 26-30 years. -: not available.

Abbreviations: F, females; M, males; GM_morph, morphological classes of *gluteus maximus*; SOL_morph, morphological classes of *soleus*. F test: Fisher's exact test of independence calculated for the morphological classes of GM (**top**) and SOL (**bottom**) entheses by sex, age classes and sex within the single age classes; *: $p < 0.05$, **: $p < 0.01$, ***: $p < 0.001$ and ****: $p < 0.0001$; NS: nonsignificant result.

Table 5. Descriptive statistical analysis (mean and standard deviation) for linear measurements of the femur and GM enthesis (**left**) and tibia and SOL enthesis (**right**) with the distinction between sex and age class (*Extended version available on Table S1, Supporting Information)*. All values are expressed in mm.

FEMUR	F			M			W	TIBIA	F			M			W
	N	Mean	SD	N	Mean	SD	test		N	Mean	SD	N	Mean	SD	test
Age class 1								**Age class 1**							
Femoral_length	6	84.7	31.7	13	67.5	7.9	NS	Tibial_length	9	58.8	26.0	12	61.8	12.9	NS
Femoral_diameter	20	7.4	1.9	27	6.2	1.5	**	Tibial_diameter	20	6.5	1.5	25	5.6	1.1	*
GM_length	8	24.4	5.7	19	20.0	4.5	NS	SOL_length	1	16.0	-	1	14.8	-	-
GM_width	19	3.2	0.8	28	3.0	0.6	NS	SOL_width	8	1.3	0.4	10	1.3	0.5	NS
Age class 2								**Age class 2**							
Femoral_length	6	165.5	28.9	3	176.0	50.0	NS	Tibial_length	5	121.2	24.7	4	141.6	33.5	NS
Femoral_diameter	12	11.4	1.9	9	11.5	1.9	NS	Tibial_diameter	11	10.1	2.0	9	10.4	1.6	NS
GM_length	9	39.5	6.4	9	34.4	6.3	NS	SOL_length	4	32.1	5.3	4	29.0	11.8	NS
GM_width	13	4.9	1.3	9	5.2	1.3	NS	SOL_width	5	2.6	0.7	4	2.3	0.8	NS
Age class 3								**Age class 3**							
Femoral_length	2	267.5	2.1	-	-	-	-	Tibial_length	1	225.0	-	1	197.0	-	-
Femoral_diameter	2	16.5	-	2	15.8	1.6	-	Tibial_diameter	1	15.4	-	2	15.4	0.3	-
GM_length	2	57.8	13.9	2	65.1	7.6	-	SOL_length	-	-	-	-	-	-	-
GM_width	2	7.3	1.3	2	7.6	0.5	-	SOL_width	-	-	-	1	2.5	-	-
Age class 4								**Age class 4**							
Femoral_length	-	-	-	3	312.3	50.9	-	Tibial_length	-	-	-	3	255.0	40.5	-
Femoral_diameter	-	-	-	4	19.7	2.6	-	Tibial_diameter	-	-	-	4	18.8	4.0	-
GM_length	-	-	-	4	78.2	13.4	-	SOL_length	-	-	-	-	-	-	-
GM_width	-	-	-	4	7.8	1.6	-	SOL_width	-	-	-	2	4.8	2.6	-
Age class 5								**Age class 5**							
Femoral_length	6	404.2	16.8	10	439.6	18.4	**	Tibial_length	6	331.7	8.6	11	364.3	20.1	**
Femoral_diameter	7	22.3	1.5	11	25.9	2.9	**	Tibial_diameter	7	19.1	1.7	10	23.1	2.2	***
GM_length	7	88.2	8.4	7	105.5	17.7	*	SOL_length	5	80.0	17.0	7	86.5	13.0	NS
GM_width	7	8.5	1.3	11	9.4	1.7	NS	SOL_width	6	4.3	0.9	10	5.6	1.0	*
Age class 6								**Age class 6**							
Femoral_length	6	419.7	9.5	9	459.0	22.5	***	Tibial_length	6	341.5	9.6	9	376.0	24.7	**
Femoral_diameter	6	23.7	2.4	9	27.7	1.8	**	Tibial_diameter	6	21.7	3.4	9	24.8	5.5	NS
GM_length	6	99.3	10.3	7	107.3	8.5	NS	SOL_length	6	78.6	12.7	7	101.5	13.8	*
GM_width	6	7.5	1.01	9	9.9	2.0	*	SOL_width	6	4.3	0.9	9	5.6	1.0	*
Age class 7								**Age class 7**							
Femoral_length	5	423.8	15.1	2	452.5	51.6	-	Tibial_length	4	339.0	22.1	2	392.0	41.0	-
Femoral_diameter	5	23.9	0.8	2	29.3	2.05	-	Tibial_diameter	5	19.7	1.4	2	23.3	1.1	-
GM_length	3	102.6	4.4	2	107.9	3.0	-	SOL_length	3	100.7	16.7	2	96.6	12.0	-
GM_width	5	8.8	1.0	2	9.1	2.3	-	SOL_width	3	4.63	0.3	2	6.1	2.6	-

Note. Age class 1: <1 year; age class 2: 1-5.9 years; age class 3: 6-10.9 years; age class 4: 11-15.9 years; age class 5: 16-20.9 years; age class 6: 21-25.9 years; age class 7: 26-30 years. -: not available.

Abbreviations: F, females; M, males; N, number of individuals; Femoral_length, maximum length of the femur; Femoral_diameter, transverse diameter at midshaft of the femur; GM_length, entheseal length of *gluteus maximus*; GM_width, entheseal width of *gluteus maximus*; Tibial_length, maximum length of the tibia; Tibial_diameter, transverse diameter at midshaft of the tibia; SOL_length, entheseal length of *soleus*; SOL_width, entheseal width of *soleus*. W: Wilcoxon rank-sum test calculated on the linear measurements of the femur and GM enthesis (left) and tibia and SOL enthesis (right) by sex within age classes; *: $p < 0.05$, **: $p < 0.01$, ***: $p < 0.001$ and ****: $p < 0.0001$; NS: nonsignificant result.

Table 6. Spearman correlation and linear regression between the morphological classes of GM (**top**) and SOL (**bottom**) and the following variables: age, linear measurements of the bones and entheses and degree of epiphyseal closure, with the distinction between the sexes.

	GM_morph					
FEMUR	**F**		**M**		**F+M**	
	ρ [a]	r^2 [b]	*ρ* [a]	r^2 [b]	*ρ* [a]	r^2 [b]
Age	0.942****	0.795****	0.916****	0.652****	0.933****	0.710****
Femoral_length	0.868****	0.595****	0.820****	0.526****	0.798****	0.548****
Femoral_diameter	0.923****	0.714****	0.913****	0.646****	0.906****	0.655****
GM_length	0.853****	0.593****	0.902****	0.602****	0.888****	0.605****
GM_width	0.868****	0.581****	0.855****	0.553****	0.848****	0.548****
Femoral_closure	0.814****	0.689****	0.795****	0.585****	0.799****	0.634****

	SOL_morph					
TIBIA	**F**		**M**		**F+M**	
	ρ [a]	r^2 [b]	*ρ* [a]	r^2 [b]	*ρ* [a]	r^2 [b]
Age	0.802****	0.596****	0.852****	0.589****	0.836****	0.579****
Tibial_length	0.759****	0.415****	0.834****	0.470****	0.819****	0.460****
Tibial_diameter	0.762****	0.455****	0.852****	0.495****	0.824****	0.485****
SOL_length	0.695***	0.286*	0.735***	0.439***	0.740****	0.405****
SOL_width	0.693****	0.287**	0.651****	0.301***	0.674****	0.315****
Tibial_closure	0.777****	0.622****	0.748****	0.587****	0.753****	0.503****

Note. *: $p < 0.05$, **: $p < 0.01$, ***: $p < 0.001$ and ****: $p < 0.0001$.

[a] Spearman's rank correlation (ρ: rho coefficient).

[b] Linear regression model (Adjusted r^2: coefficient of determination).

Abbreviations: F, females; M, males; GM_morph, morphological classes of *gluteus maximus*; SOL_morph, morphological classes of *soleus*; Femoral_length, maximum length of the femur; Femoral_diameter, transverse diameter at midshaft of the femur; GM_length, entheseal length of *gluteus maximus*; GM_width, entheseal width of *gluteus maximus*; Tibial_length, maximum length of the tibia; Tibial_diameter, transverse diameter at midshaft of the tibia; SOL_length, entheseal length of *soleus*; SOL_width, entheseal width of *soleus*; Femoral_closure, degree of epiphyseal closure of the femur; Tibial_closure, degree of epiphyseal closure of the tibia.

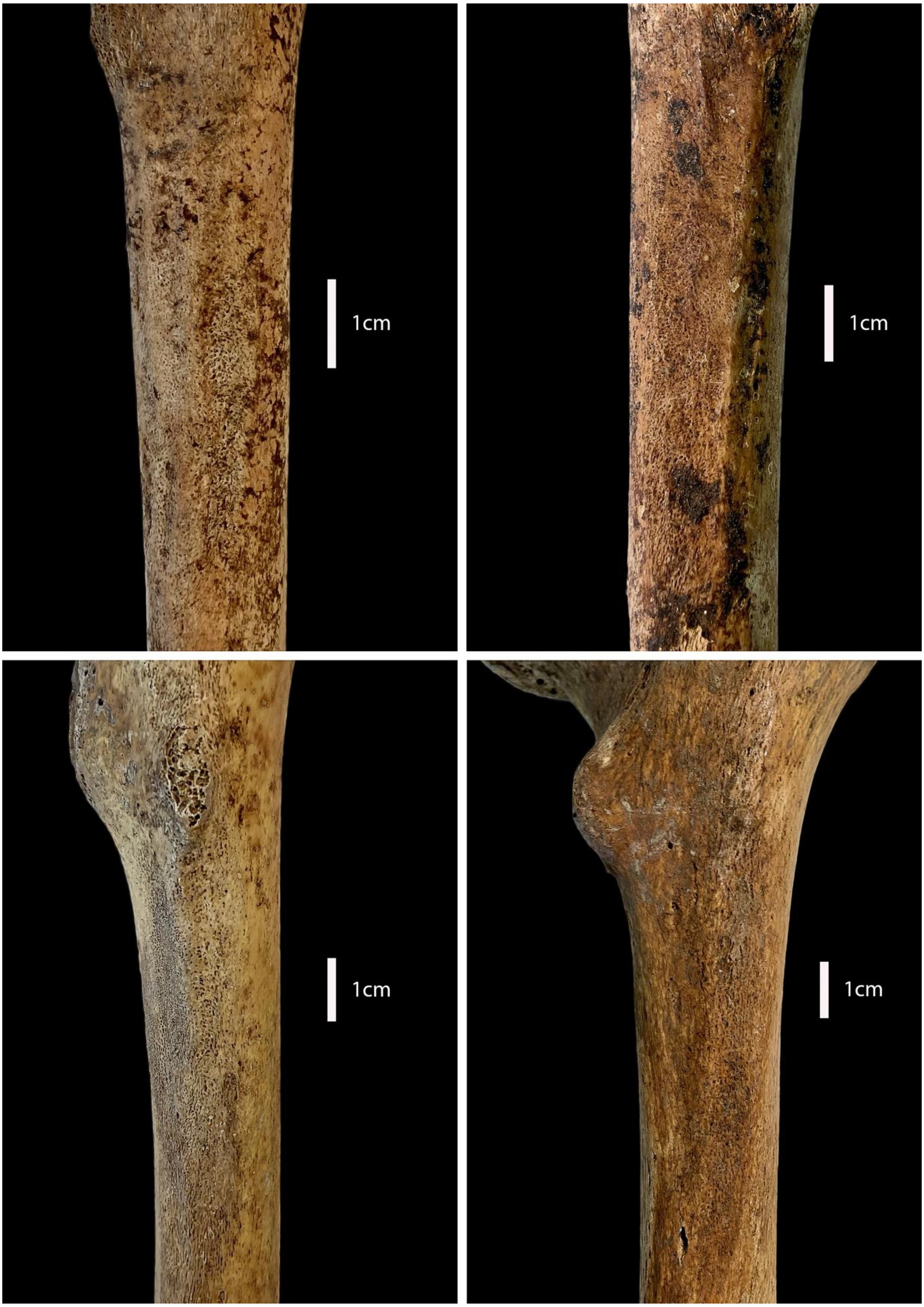

Figure 1. Examples of GM1: fine porosity. **Top left**: BO5 B100 right (F, age class 2), with a fossa**. Top right**: BO6 A337 left (M, age class 3). **Bottom left**: BO50 C4511 right (M, age class 5), with a third trochanter. **Bottom right**: BO98 D6296 right (F, age class 5), with a fossa.

Figure 2. Examples of GM2: furrowed surface. **GM2a** on top: neatly oriented furrows; **GM2b** on bottom: randomly oriented furrows. **Top left**: BO29 A298 right (M, age class 1), with a fossa; **Top right**: BO61 B120 left (F, age class 1); **Bottom left**: BO62 B8124 right (F, age class 2), with a fossa; **Bottom right**: BO20 A273 right (M, age class 2), with a fossa.

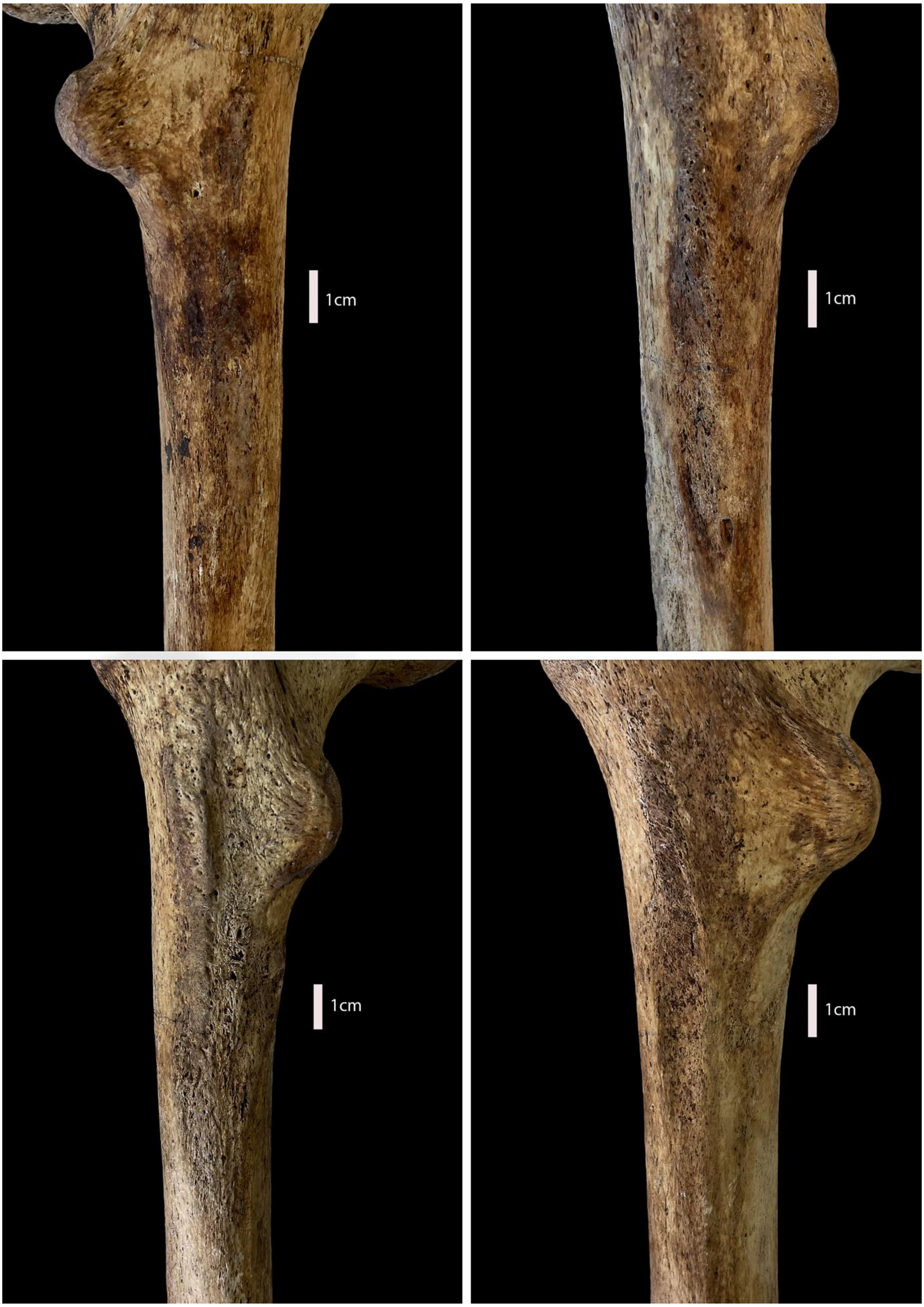

Figure 3. Examples of GM3: mixed morphology formed by mineralized tissue formations and a rather smooth surface defined by a fine porosity or smooth furrows. A proximal-distal pattern of development is recognizable in all four photos, although presenting different degrees of extension of the mineralized tissue. **Top left**: BO25 D5685 right (F, age class 5); **Top right**: BO29 D5921 left (F, age class 6), with a fossa and woven bone covering the mineralized tissue formations**; Bottom left**: BO30 C4564 left (M, age class 6), with a fossa; **Bottom right**: BO51 C4750 left (M, age class 5), with a fossa and woven bone covering the mineralized tissue formations.

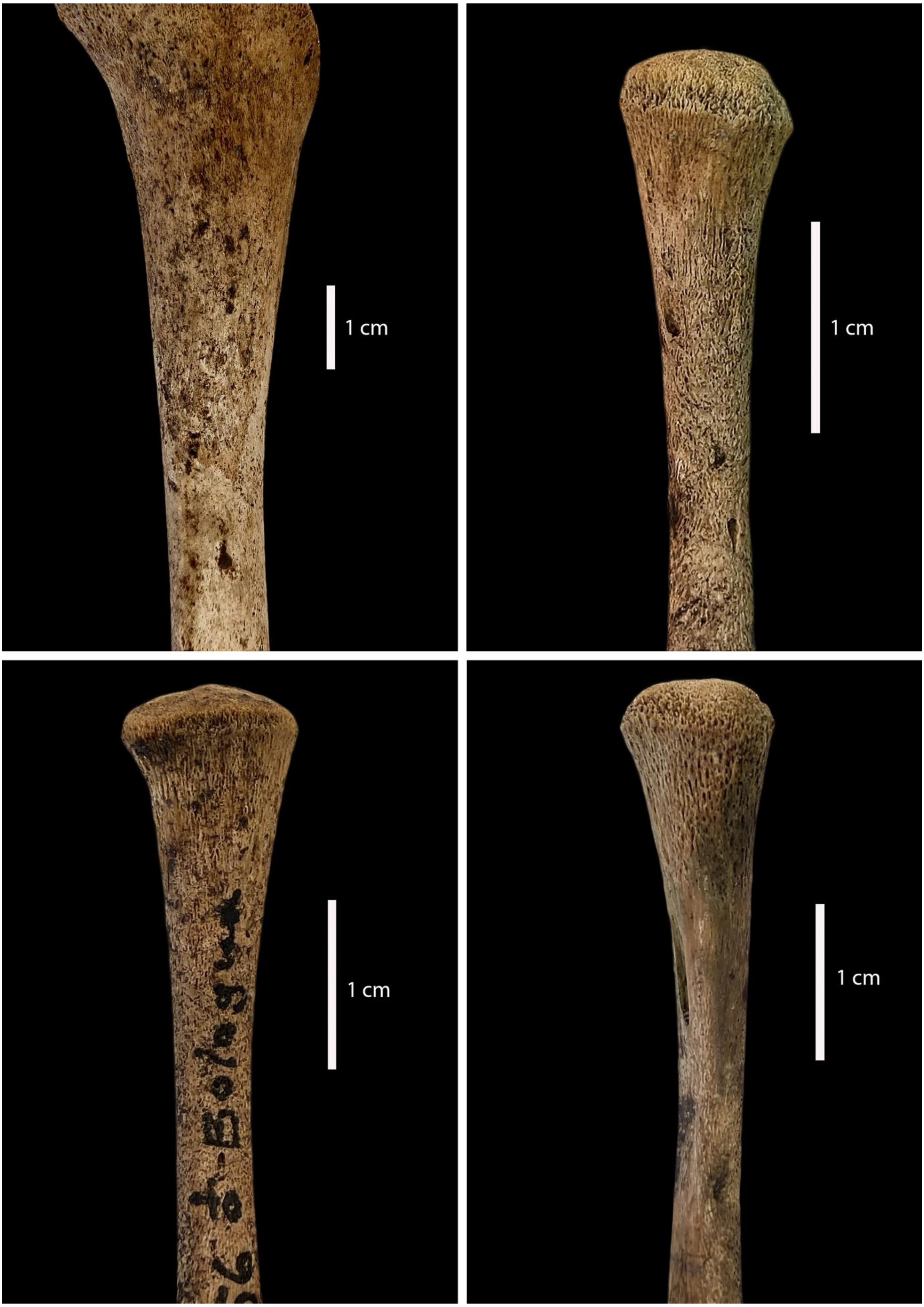

Figure 4. Examples of SOL1. The enthesis is totally indistinguishable from the surrounding bone. **Top left**: BO4 A213 right (M, age class 2); **Top right**: BO47 A303 left (M, age class 1); **Bottom left**: BO56 A338 right (M, age class 1); **Bottom right**: BO66 A318 left (M, age class 1).

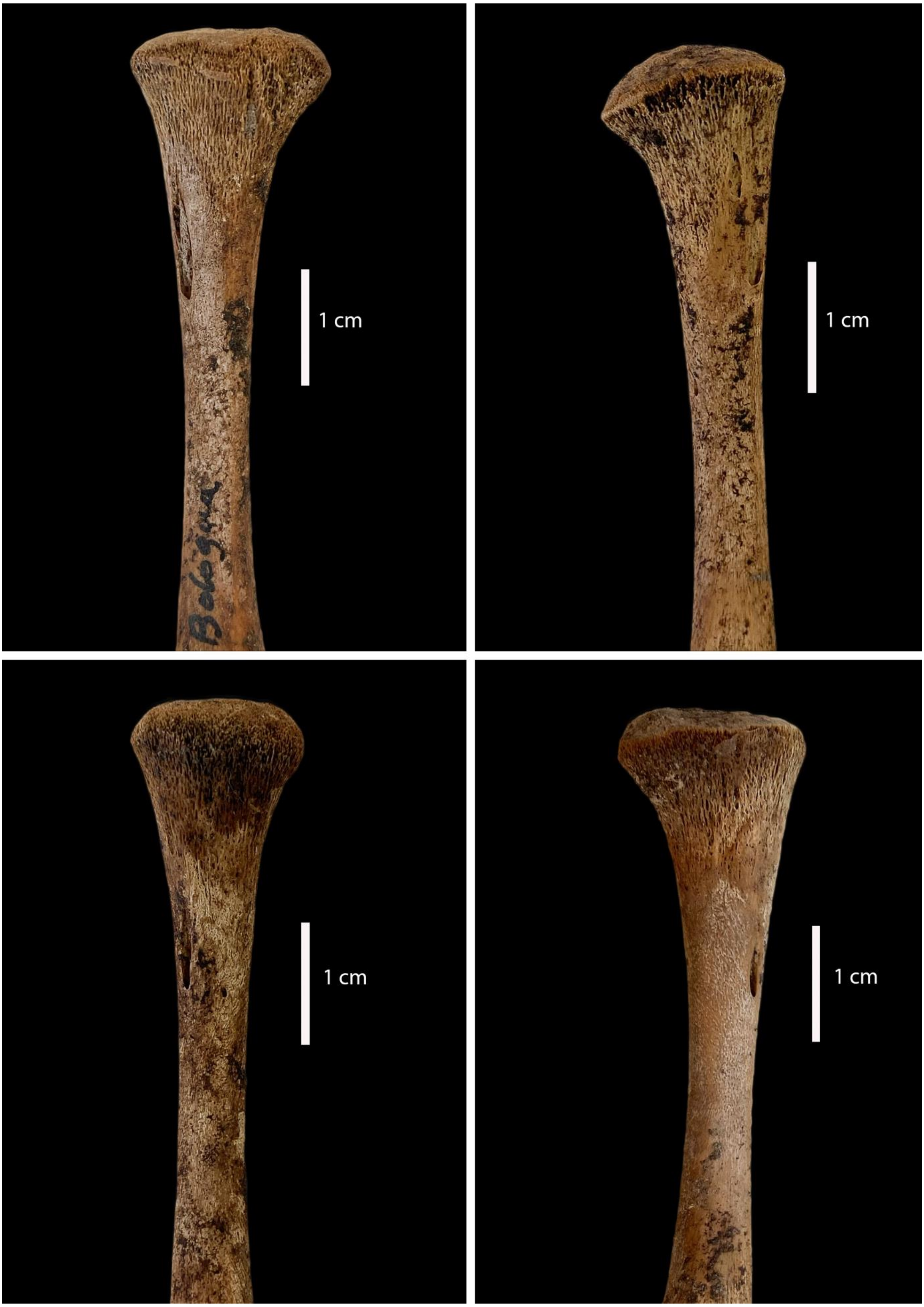

Figure 5. Examples of SOL2. The enthesis appears only as a line with no width. **Top left**: BO27 B96 left (F, age class 1); **Top right**: BO33 A296 right (M, age class 1); **Bottom left**: BO40 A324 left (M, age class 1), with a fossa; **Bottom right**: BO45 B101 left (F, age class 1).

Figure 6. Examples of SOL3. The enthesis shows a discontinuous surface characterized by furrowed surface with furrows that may or may not frame oval-shaped pores. **Top left**: BO3 B8111 left (F, age class 3), with a fossa; **Top right**: BO9 A289 left (M, age class 3), with a fossa, the furrows enclose oval-shaped pores; **Bottom left**: BO55 B8059 left (F, age class 1), with a fossa; **Bottom right**: BO67 A310 right (M, age class 1), the furrows enclose oval-shaped pores.

Figure 7. Examples of SOL4. Mixed morphology between a longitudinal protrusion and finely porous/furrowed surface. **Top left**: BO70 D4785 left (F, age class 6), with a fossa and a distal-proximal pattern of development (a layer of woven bone partly covers the longitudinal protrusion); **Top right**: BO99 D5809 left (F, age class 5), with a fossa and woven bone partly covering the longitudinal protrusion; **Bottom left**: BO75 C4848 left (M, age class 6), with a fossa; **Bottom right**: BO96 C1514 right (M, age class 6), with a fossa and a distal-proximal pattern of development (a layer of woven bone fully covers the longitudinal protrusion).

Figure 8. Boxplots representing the distribution of the individuals by age within each morphological class assigned to the GM (**top**) and SOL (**bottom**) entheses and divided by sex.

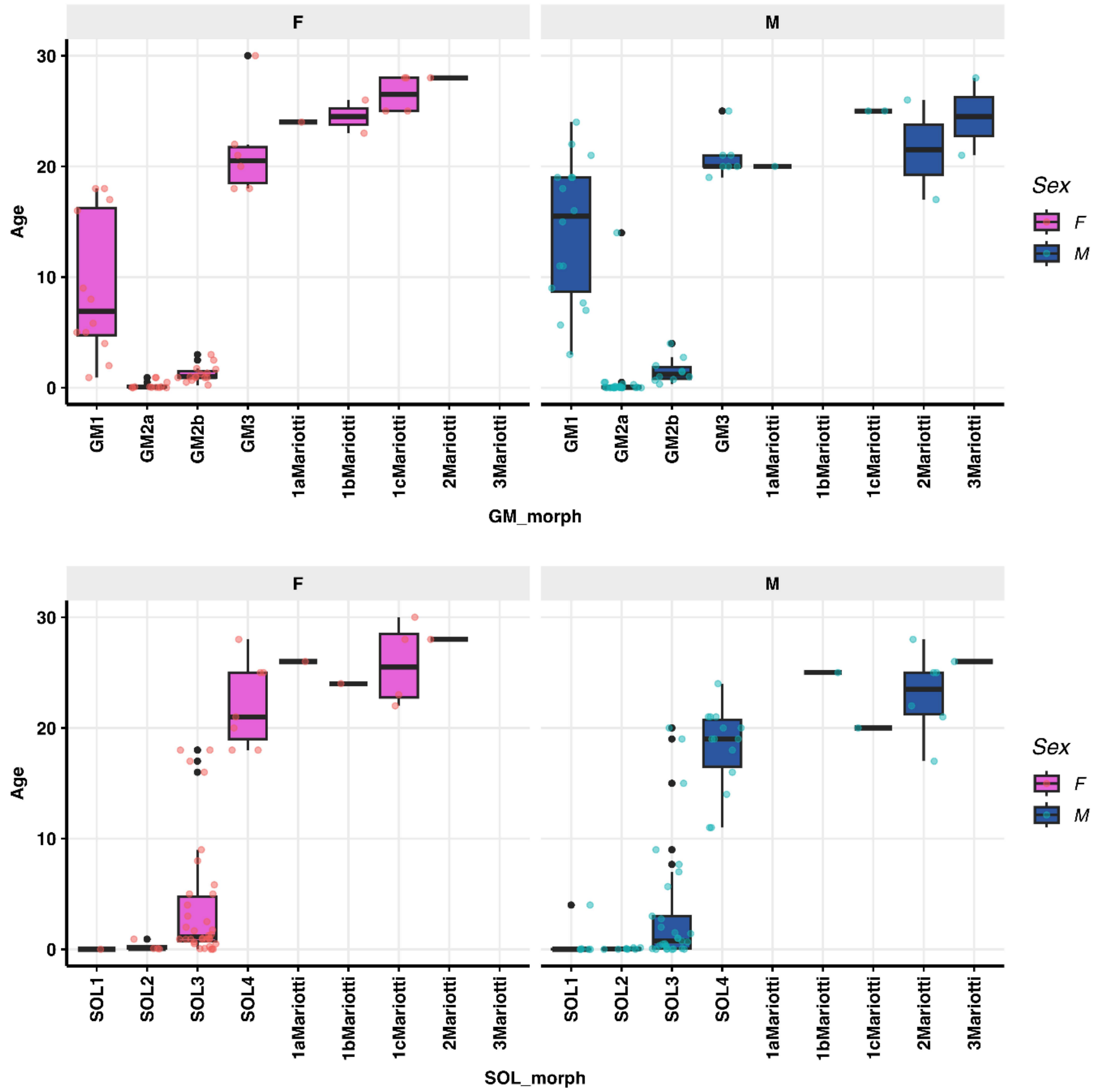

Abbreviations: F, females; M, males.

Figure 9. FAMD relating to GM enthesis (**top row**) divided by morphological classes (**a**), sex (**b**), degree of epiphyseal closure of the femur (**c**) and FAMD relating to SOL enthesis (**bottom row**) divided by morphological classes (**d**), sex (**e**), degree of epiphyseal closure of the tibia (**f**). Please refer to the online version of this article for color interpretation.

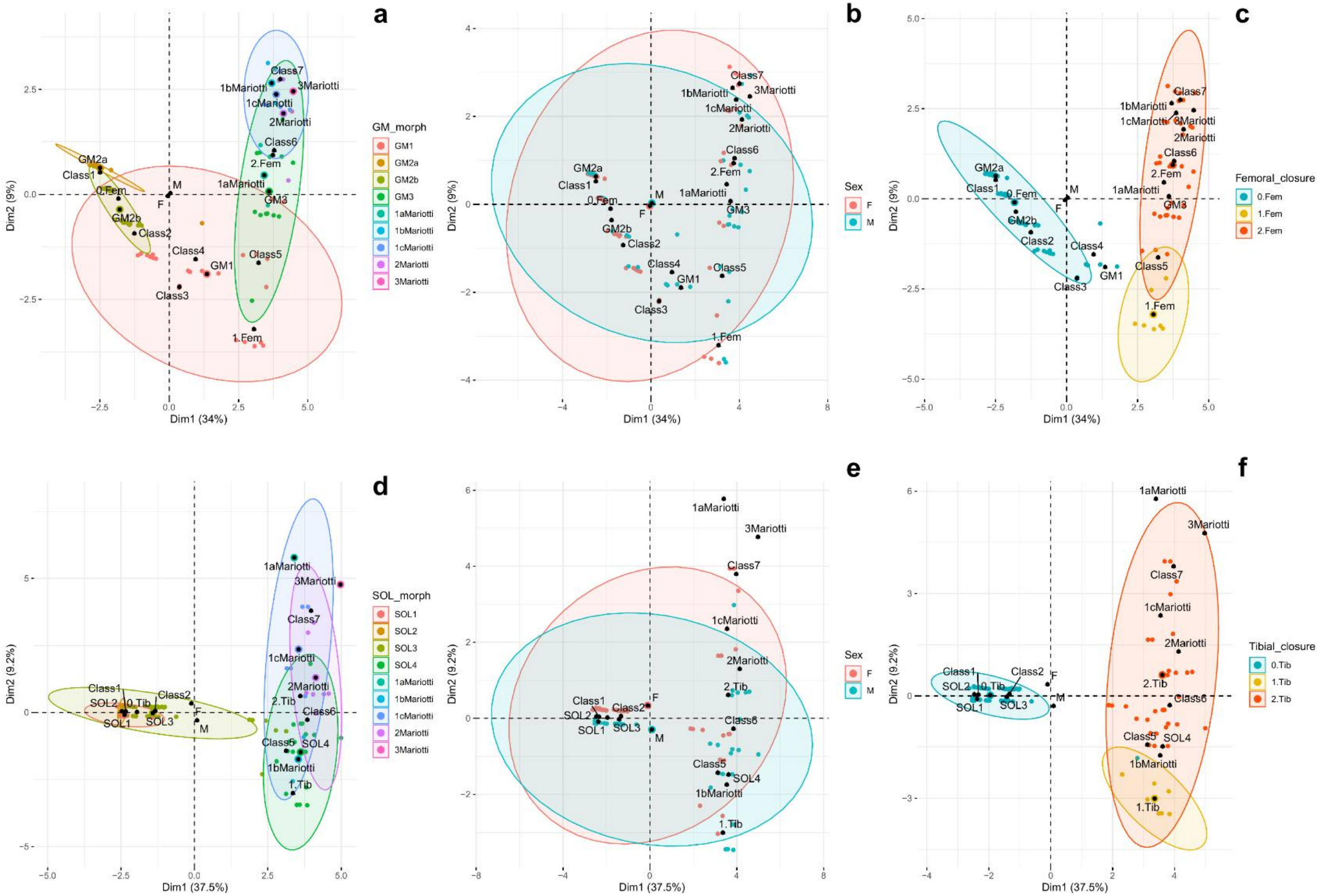

Abbreviations: F, females; M, males. GM_morph, morphological classes of *gluteus maximus*; SOL_morph, morphological classes of *soleus*. Femoral_closure, degree of epiphyseal closure of the femur; Tibial_closure, degree of epiphyseal closure of the tibia (0.Fem/0.Tib: unfused epiphyses, 1.Fem/1.Tib: partial state of closure, 2.Fem/2.Tib: total state of closure). Class1, age class 1 (<1 year); Class2, age class 2 (1-5.9 years); Class3, age class 3 (6-10.9 years); Class4, age class 4 (11-15.9 years); Class5, age class 5 (16-20.9 years); Class6, age class 6 (21-25.9 years); Class7, age class 7 (26-30 years).